Spatiotemporal dynamics of soil erosion response to environmental drivers in Maracas Valley, Trinidad and Tobago: A RUSLE and NDVI-Based Analysis

Janae Steadman

August 2024

MSc Geographical Information Systems
School of Geography, University of Leeds

A dissertation submitted in partial fulfilment of the requirements of the Masters Degree in Geographic Information Systems of the University of Leeds

Abstract

Soil erosion is a critical environmental challenge, particularly in regions experiencing rapid land use changes and shifting climatic conditions. The Maracas Valley region of Trinidad and Tobago

is a socially and ecologically significant area, characterised by diverse habitats containing the Maracas-St. Joseph river which supplies 80% of the country's water supply. Increasing urbanisation and deforestation has resulted in significant land cover change in the region, resulting in severe environmental degradation. The purpose of this study is to quantify the spatiotemporal patterns of soil erosion in the Maracas Valley using the Revised Universal Soil Loss Equation and to identify the drivers of soil erosion in the region.

RUSLE *(A)* is computed with 5 factors: rainfall erosivity (*R*), soil erodibility (*K*), slope length and steepness factor (*LS*), cover management factor (*C*) and conservation practice factor (*P*). The analysis revealed that soil erosion in the Maracas Valley has declined considerably from 1990 to 2020, primarily as a result of reforestation in the region with mean soil erosion values declining from 266.885 t ha^{-1} y^{-1} to 59.491 t ha^{-1} y^{-1}. Cover management and Soil Erodibility were identified as the most significant contributors to the variability in soil erosion across the study area. The findings underscore the critical role of sustainable land management practices, particularly reforestation and soil conservation techniques, in mitigating soil erosion. This study provides valuable insights into the effectiveness of ongoing reforestation efforts and highlights the need for continued focus on conservation practices to preserve the ecological integrity of the Maracas Valley, which is vital for the region's water security and biodiversity.

Acknowledgements

I would like to express my gratitude to my supervisor, Dr. Liam Taylor for his invaluable guidance and support throughout this research project. His expertise and encouragement have

helped me tremendously to complete this research. I would also like to thank Dr. Paul Norman for his thought-provoking lectures, which have encouraged me to think critically about research. Lastly, I would like to extend my gratitude to my classmates, friends and family for their unwavering support throughout the year.

Table of Contents

1. Introduction

Soil erosion is the process by which fertile topsoil is displaced from the soil's surface. This phenomenon is dependent on natural forces such as rainfall intensity, wind and soil physical properties (Borrelli et al., 2021). While these natural factors play a critical role, anthropogenic activities have increasingly exacerbated soil erosion rates worldwide. Rapid population growth, urbanisation, deforestation, and changes in land use have led to unprecedented levels of soil loss threatening agricultural productivity, water quality, and ecosystem stability (Nel et al., 2013).

Prior to 1970, in Maracas Valley, Trinidad, land use was predominantly agricultural. Residents engaged in farming, growing cash crops and vegetables with estates varying in size from small plots to large areas exceeding 300 acres (Maracas Valley Action Committee, 2010).However, from the mid-1960s, large agricultural estates were subdivided into smaller residential plots, leading to rapid urbanisation and population growth. By 2005, Maracas Valley's population increased by 135%. Facilitating this drastic population increase, the valley also saw a 250% rise in the number of buildings, a 225% expansion of the road network as well as a 283% increase in quarrying operations. Concurrently, the area experienced a 17.5% loss in forest cover (Maracas Valley Action Committee, 2010).

The transition from a predominantly agricultural landscape to a more urbanised environment has had extensive implications for soil stability and erosion. Impervious surfaces, associated with urbanisation, such as buildings and roadways, reduce the natural infiltration of rainwater into the soil, leading to increased surface runoff and erosion (Strohbach et al., 2019). The expansion of the road network not only facilitated greater human activity and mobility but also altered natural drainage patterns, contributing to the acceleration of soil erosion (Maracas Valley Action Committee, 2010). Additionally, the increase in quarrying activities has further exacerbated soil erosion. Quarrying disturbs both soil and rock layers, which can lead to a significant increase in the amount of sediment that is washed into nearby water bodies during rainfall events; clogging waterways, increasing turbidity, and reducing water quality (Babalwa Kafu-Quvane and Sanelisiwe Mlaba, 2024). The physical disturbance of the land from quarrying also destabilises the surrounding landscape, resulting in more severe erosion and landslides over time, particularly in areas with steep slopes (Darwish et al., 2010).

The environmental consequences of these changes have been exhaustive, both globally and within the study area, resulting in more frequent and severe flooding events, increased pollution and sedimentation, decline in lotic ecosystem stability as well as increased landslides caused by destabilised slopes (Fontes De Maria and Phillips, 2019; Maracas Valley Action Committee, 2010). In response to these changes in Trinidad and Tobago, the National Reforestation and Watershed Rehabilitation Programme (NRWRP) was established in 2000 to address the environmental impacts of urbanisation and industrialization and the Maracas Valley Action Committee (MVAC) was established in 2002 to facilitate community action and education as well as communication between the community and policymakers for sustainable development. NRWRD and MVAC have played a crucial role in reforestation efforts aimed at restoring lost forest cover and restabilising soil.

While much attention has been given to the environmental challenges posed by urbanisation and quarrying, the extent and severity of soil erosion has not been adequately quantified. Moreover, the impact of land cover changes, including deforestation and subsequent reforestation efforts, on soil erosion rates remains underexplored. Thus, there is a critical need for further research and analysis to better understand soil erosion dynamics in the region.

To address these challenges, this study utilises the Revised Universal Soil Loss Equation (RUSLE), a widely used mathematical model for the estimation of soil erosion based on factors such as rainfall, soil erodibility, topography, and land cover. The ability of RUSLE to be applied in various contexts, its ability to integrate diverse data sources and its undemanding computation makes it an effective tool for quantifying soil erosion, particularly in regions with limited data availability such as Trinidad and Tobago. Due to the lack of comprehensive historical data, this study focuses on the period from 1990 to 2020, to quantify soil erosion and assess the influence of land cover changes and other contributing environmental drivers on soil erosion rates in Maracas Valley.

Specifically, this study aims to determine the spatial and temporal patterns of soil erosion in the Maracas Valley from 1990 to 2020 using the Revised Universal Soil Erosion. Then, to assess how land cover changes and other environmental drivers have influenced soil erosion rates and finally, to explore the implications of the identified soil erosion patterns for soil and water conservation strategies in the region.

2. Literature Review

Soil erosion modelling seeks to develop quantitative representations of the mechanisms that govern the transportation and deposition of soil particles (Ghosal and Das Bhattacharya, 2020). Since the early 1940s, the field of geomorphology has seen an expansion in the development of soil erosion models; evolving from simple empirical models to more complex, process-based models (Ejaz et al., 2023). Zingg (1940) developed the first model for soil loss estimation, exploring the relationship between erosion and land slope and length. Further exploration of this work led to the Universal Soil Loss Equation (USLE) in 1960 and subsequent models such as the Revised Universal Soil Loss Equation (RUSLE) and the Water Erosion Prediction Project (WEPP) (Ghosal and Das Bhattacharya, 2020). The aim of this literature review is threefold; to provide an assessment of the methods of modelling soil erosion, to explore the components of the RUSLE model in various studies across different geographic regions and land use contexts and to review how changes in land use influence soil erosion rates as quantified by RUSLE.

2.1 Quantifying Soil Erosion

While there are many soil erosion models and applications of these models today, they are not universally applicable. The choice of the most suitable model would be dependent upon various factors including the intended use of the model, study area characteristics, data availability, the model's data prerequisites, the accuracy and reliability of the model, as well as any underlying assumptions (Luvai et al., 2022). The Sediment Delivery Distributed Model (SDD) (Ferro and Porto, 2000), the Water Erosion Prediction Project (WEPP) (Laflen et al., 1991), the Universal Soil Loss Equation (USLE) (Wischmeier and Smith, 1978) and the Revised Universal Soil Loss Equation (RUSLE) (Renard et al., 1997) are some of the most widely used erosion models (Borrelli et al., 2021).

The WEPP model provides detailed, site-specific simulation of soil erosion processes, accounting for complex interactions between rainfall, soil characteristics, topography, and land management practices (Laflen et al., 1991). However, its complexity and extensive data requirements can limit its accessibility and practical application in regions with sparse data (Luvai et al., 2022). Conversely, SDD provides a straightforward approach to estimating soil loss

using basic input parameters and simple equations, making it particularly useful in regions with limited data availability (Renard et al., 1997). While it may not capture the fine-scale variability in areas with complex landscapes or diverse land uses, the SDD model serves as an efficient and practical tool for initial evaluations and broad-scale analyses. (Ferro and Porto, 2000).

2.2 Analysis of RUSLE factors

The USLE and its revised version RUSLE have been extensively utilised to predict soil erosion in regions where empirical data is scarce while maintaining a similar level of accuracy as the more advanced and data intensive models (Sourn et al., 2022). The development of RUSLE was driven by the need to improve upon the original USLE model by incorporating additional data and resources. RUSLE maintains the same basic formula as USLE but includes several enhancements, including new approaches to assessing soil erodibility and cover management, new equations to account for slope length and steepness as well as updated support practice values (Renard et al., 1997). RUSLE assesses annual soil loss (A) by incorporating five factors; rainfall erosivity (R), soil erodibility (K), slope length and slope steepness (LS), cover management (C), and support practice (P). Researchers have then further developed techniques for estimating these factors, each adapted to different environmental conditions and data availability (Ghosal and Das Bhattacharya, 2020). As a result, RUSLE remains a principal model for soil erosion studies, bridging the gap between theoretical research and practical application.

Geographical Information Systems (GIS) and remote sensing serve as critical tools in environmental research, facilitating the collection and analysis of spatial data to model and predict soil erosion patterns effectively (Tsihrintzis et al., 1996). According to Negese et al. (2021) integrating both remote sensing and GIS with soil erosion models can be particularly beneficial. The application of RUSLE in a GIS framework has been employed in various studies spanning a large geographical extent; Brazil (Lu et al., 2004; Rodrigues et al., 2017), Ethiopia (Kebede et al., 2021; Amsalu and Mengaw, 2014; Getu et al., 2022), Saudi Arabia (Mallick et al., 2014; Ejaz et al., 2023), Kazakhstan (Darbayeva et al., 2020) and Italy (Gianinetto et al., 2019 ;Stanchi et al., 2014). Thus, the RUSLE model is not only accessible to a wide range of users, it

is applicable to large spatial and temporal contexts making it one of the most principal soil erosion models.

2.2.1 Rainfall Erosivity (R factor)

Rainfall erosivity quantifies the effect of raindrop impact on soil erosion (Nearing et al., 2017). The original equation of *R*, based on Wischmeier and Smith (1978), assesses the kinetic energy of rain and requires measurements of rainfall intensity. Researchers have since refined this methodology and developed various methods of calculation to account for the unique rainfall patterns and intensity specific to different climates. Yu and Rosewell (1996) designed for the subtropical climates of Australia, incorporating daily rainfall data and storm event intensity while Panagos et al. (2015) developed an equation for European climates, incorporating a pan-European rainfall erosivity dataset for more precise regional calculations. Due to the lack of data availability in developing countries, Hurni (1985) developed an equation, utilising convenient annual average rainfall data while Lujan and Gabriels (2005) and Nel et al. (2013) have addressed this challenge by utilising the Modified Fournier Index (Arnoldus 1980). This index estimates the rainfall erosivity factor using more readily available monthly and annual precipitation data, making it a practical alternative for regions with limited access to rainfall intensity records (Arnoldus 1980).

2.2.2 Soil Erodibility (K factor)

Soil Erodibility represents the susceptibility of soil to erosion under the impact of rainfall and runoff; influenced by soil texture, structure, and organic matter content (Martínez-Murillo et al., 2020). Different *K* factor algorithms have been developed and applied based on suitability and requirement. Wischmeier and Smith's (1978) model incorporates soil texture, organic matter content, soil structure, and permeability. El-Swaify and Dangler (1976) developed a model considering grain size distribution and the degree of saturation of the soil which was further supported by Hurni (1985) who then incorporated soil colour and type. Loch and Rosewell (1992) developed a model for Australian soils, focusing on soil aggregate stability and dispersion characteristics while Renard et al. (1997) proposed an empirical equation based on the geometric mean particle diameter of soil. In many developing countries, similar to rainfall data, detailed

soil data is often unavailable or difficult to obtain. Williams and Sharpley (1990) proposed an equation that makes use of easily available data points, limiting the requirements of the equation to sand content (%), silt content (%), clay content (%), and soil organic content (%), making it particularly suitable for these regions.

2.2.3 Slope Length and Steepness (LS factor)

The slope length and steepness factor (LS) quantifies the influence of topography on erosion rates (Luvai et al., 2022). Various methods have been developed to calculate the LS factor, each considering different characteristics of slope length and gradient. With GIS-RUSLE integration and widely available Digital Elevation Models, calculating the LS factor is relatively accessible and straightforward. McCool et al. (1987) proposed an LS factor equation adapted for steep slopes, often used in mountainous regions where slope steepness significantly influences erosion while Liu et al. (2000) Created a method for estimating the LS factor for agricultural fields in China, integrating local topographic and soil data to enhance model precision. Moore and Burch (1986) introduced a more complex approach that integrates flow accumulation and cell size to determine the LS factor, providing improved accuracy for complex terrains and wider applicability across regions.

2.2.4 Cover Management (C factor)

The cover management (*C*) factor quantifies how different types of vegetation, crop cover, and land management practices influence the rate of soil erosion by affecting factors like soil protection, runoff, and infiltration. The original RUSLE model provided a set of standard C values based on different types of vegetation and land management practices, including crops, pastures, and forest cover (Wischmeier and Smith 1978). Recently, numerous methodologies have been developed utilising the Normalised Differential Vegetation Index (NDVI) to estimate C (De Jong, 1994; Valor, 1996). Durigon et al. (2014) developed a methodology proposing the inverse relationship between NDVI and C Factor, such that higher NDVI values, reflecting denser vegetation, correspond to lower C values, indicating reduced soil erosion potential.

2.2.5 Support Practice (P factor)

Support practice (*P*) is regarded as one of the most uncertain factors of the RUSLE model and the traditional concept by Wischmeier and Smith is still one of the most widely used methods for computing the P factor (Luvai et al., 2022). This involves pre-determined P values assigned to different types of support practices such as terracing and contouring. Additionally, various studies (Kidane et al., 2019; Gelagay, 2016; Kogo et al., 2020) utilise the approach developed by Hurni (1985) wherein land use and land cover are classified as either ‘cultivated’ or ‘other’ under the foundational presumption that conservation strategies are effectively implemented on cultivated land.

2.3 Land use and soil erosion

Quantifying soil erosion under land use changes is essential for developing conservation strategies to intercept and reduce soil and water degradation and to ensure sustainable agricultural productivity (Qiao et al., 2023). Moisa et al. (2021) utilised RUSLE to evaluate soil erosion in the Temeji watershed in Western Ethiopia, revealing significant increases in erosion rates following the conversion of grassland and forested areas to agricultural land with 54.4% of the study area categorised under severe erosion. Similarly, Thapa (2020) applied the RUSLE model to assess the effects of urbanisation on soil erosion in the Dokha District of Nepal, finding that impervious surfaces significantly exacerbated soil loss due to increased runoff and reduced infiltration. However, there is a significant gap in research concerning the application of RUSLE in tropical environments. Given the distinct environmental conditions, such as high rainfall intensity and diverse land cover, further research is essential to adapt and validate the RUSLE model for these unique settings (Harliando et al., 2022). Addressing this gap is crucial for developing targeted soil and water conservation strategies that are tailored to the specific challenges of tropical ecosystems.

2.4 NDVI as a Measure of Land Cover

The Normalised Difference Vegetation Index (NDVI) is a remote sensing metric used to assess vegetation health and cover by comparing near-infrared and red reflectance values from satellite

imagery (Xue and Su, 2017). Its ability to provide consistent and comparable data across diverse landscapes makes it an essential tool for understanding vegetation dynamics. Thus, several studies have utilised NDVI as a means of quantifying land cover and assessing land cover change within various scales and climates (Aburas et al., 2015; Defries and Townshend, 1994; Usman et al., 2015; Morawitz et al., 2006).

While NDVI-derived land cover classifications have been valuable for understanding vegetation patterns, integrating NDVI with soil erosion models like RUSLE offers a new approach to evaluate how changes in land cover influence soil erosion rates (Durigon et al., 2014). Although direct studies combining NDVI with RUSLE are limited, existing research has shown that areas with high vegetation cover, as identified through traditional land cover classification and RUSLE methods, generally exhibit lower soil erosion rates (Sharma et al., 2010; Kavian et al., 2016; Moisa et al., 2021). In studies where NDVI was used separately to assess vegetation cover, findings consistently indicated that higher vegetation density correlates with reduced soil erosion due to increased soil protection and reduced runoff (Ouyang et al., 2010; Zhou et al., 2008). By combining NDVI-based land cover data with the RUSLE model, researchers can gain a more nuanced understanding of how changes in vegetation cover affect soil erosion dynamics.

3. Methodology

3.1 Research Approach

Soil erosion modelling is an essential component in understanding and mitigating the effects of soil loss. Various empirical and process-based models have been proposed and utilised to evaluate and predict soil hazard zones. The RUSLE model was selected due to its applicability in a wide range of contexts and flexibility in data sources; facilitating accurate soil erosion estimates with limited data availability.

3.2 Study Area

3.2.1 Location and Extent

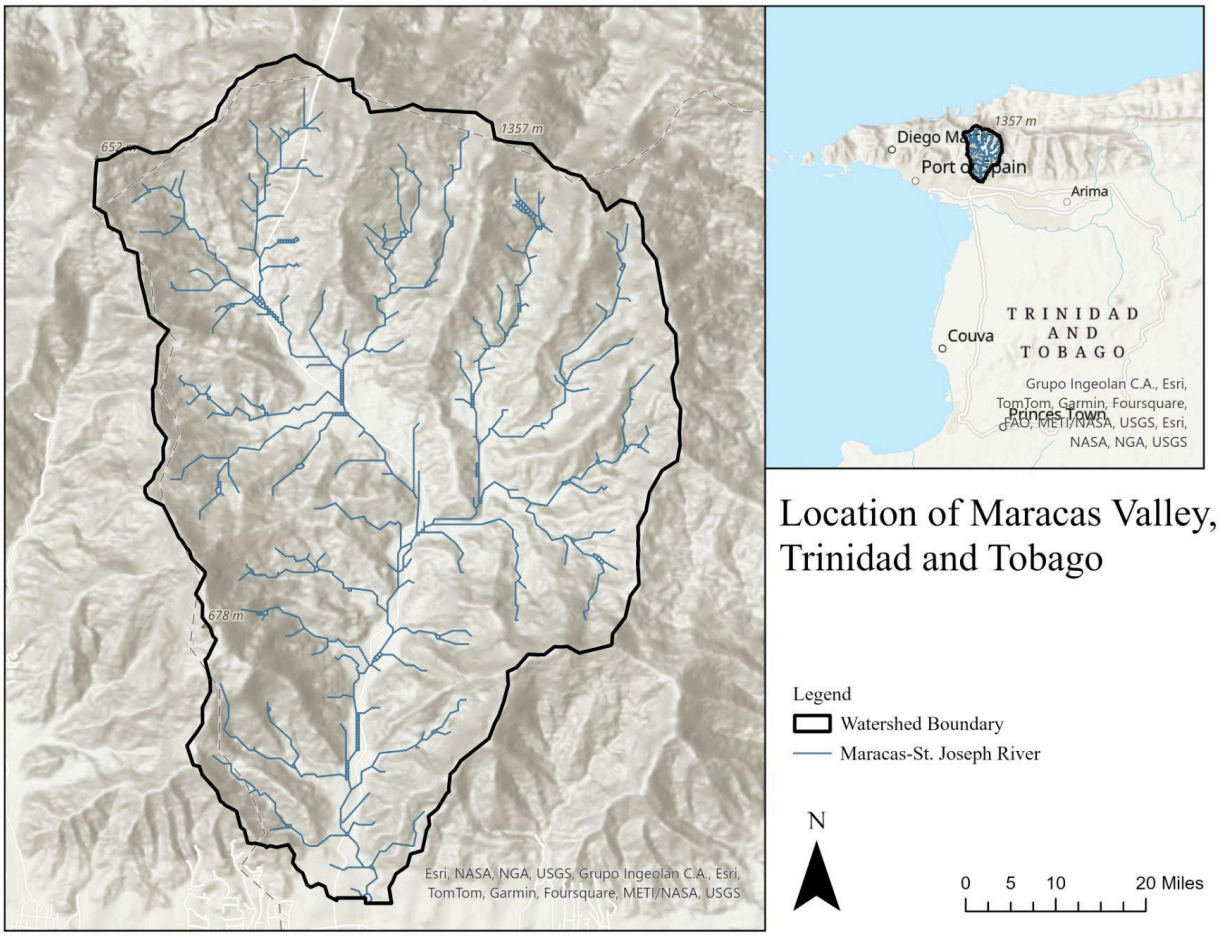

Figure 1. Location of the Study Area

The Maracas Valley lies at the foothills of the Northern Range of Trinidad, the major island in the Republic of Trinidad and Tobago and the southernmost island in the Caribbean (Singh, 1997). It lies between 10° 39’ to 10° 44’ N latitudes and 61° 23’ and 61° 26’ W longitudes and is one of the numerous valleys that constitute the Northern Range’s watershed area, which supplies approximately 80% of the water supply of Trinidad (The Maracas Valley Action Committee, 2010). The Maracas-St. Joseph River is supplied by the Loango tributary and the Acono tributary, flowing from the northwest and east respectively with dense forest concentrated in the upper catchment and increasing urbanisation in the lower catchment (Ragoobir, 2018).

Trinidad and Tobago's climate is marked by two distinct wet and dry seasons. The Tropical Marine Climate, representative of the dry season, runs from January to May and the Modified Moist Equatorial Climate which defines the wet season runs from June to December (Trinidad and Tobago Meteorological Service, 2024). The average annual rainfall is estimated to be between 1800mm and 3000mm with averages over 200 mm or more from the onset of the wet season. Temperatures range between 26°C and 32°C annually, with minimal variation throughout the year (Trinidad and Tobago Meteorological Service, 2024).

Maracas Valley's terrain can be characterised by steep slopes with over 60% of the Maracas-St. Joseph catchment having slopes over 30% (Jaramillo et al., 2007). Urban areas are primarily centred around the gentle slopes around the Maracas-St.Joseph river and the alignment of the Maracas Royal Road (The Maracas Valley Action Committee, 2010).

3.3 Data collection

The evaluation of soil erosion using the Revised Universal Soil Loss Equation is grounded in its component factors which include inputs such as digital elevation models (DEM), rainfall data, soil type data, and satellite imagery. These data were sourced from various organisations, including the United States National Aeronautics and Space Administration (NASA), the Trinidad and Tobago Meteorological Service, the Food and Agriculture Organisation (FAO), and the United States Geological Survey (USGS). Given that these data sources differ in format, projection, quality, and resolution, thorough evaluation and preprocessing are essential and recognising the inherent uncertainties that these variations introduce into the model is crucial for producing and interpreting accurate results.

3.3.1 Terrain

The ASTER Global Digital Elevation Model (GDEM) Version 003 (NASA et al., 2019), was used to extract the terrain data needed for the RUSLE model. The extracted DEM was used to derive several key terrain parameters necessary for the RUSLE model:

- Flow Length: Measures the length of the flow path from a given point on the terrain to the outlet (Zhang et al., 2017).

- Flow Direction: Identifies the direction in which water flows across the surface.
- Flow Accumulation: Represents the accumulation of flow from upstream cells, indicating areas of high water concentration and potential erosion (Zhang et al., 2017).
- Slope: Measures the steepness of the terrain

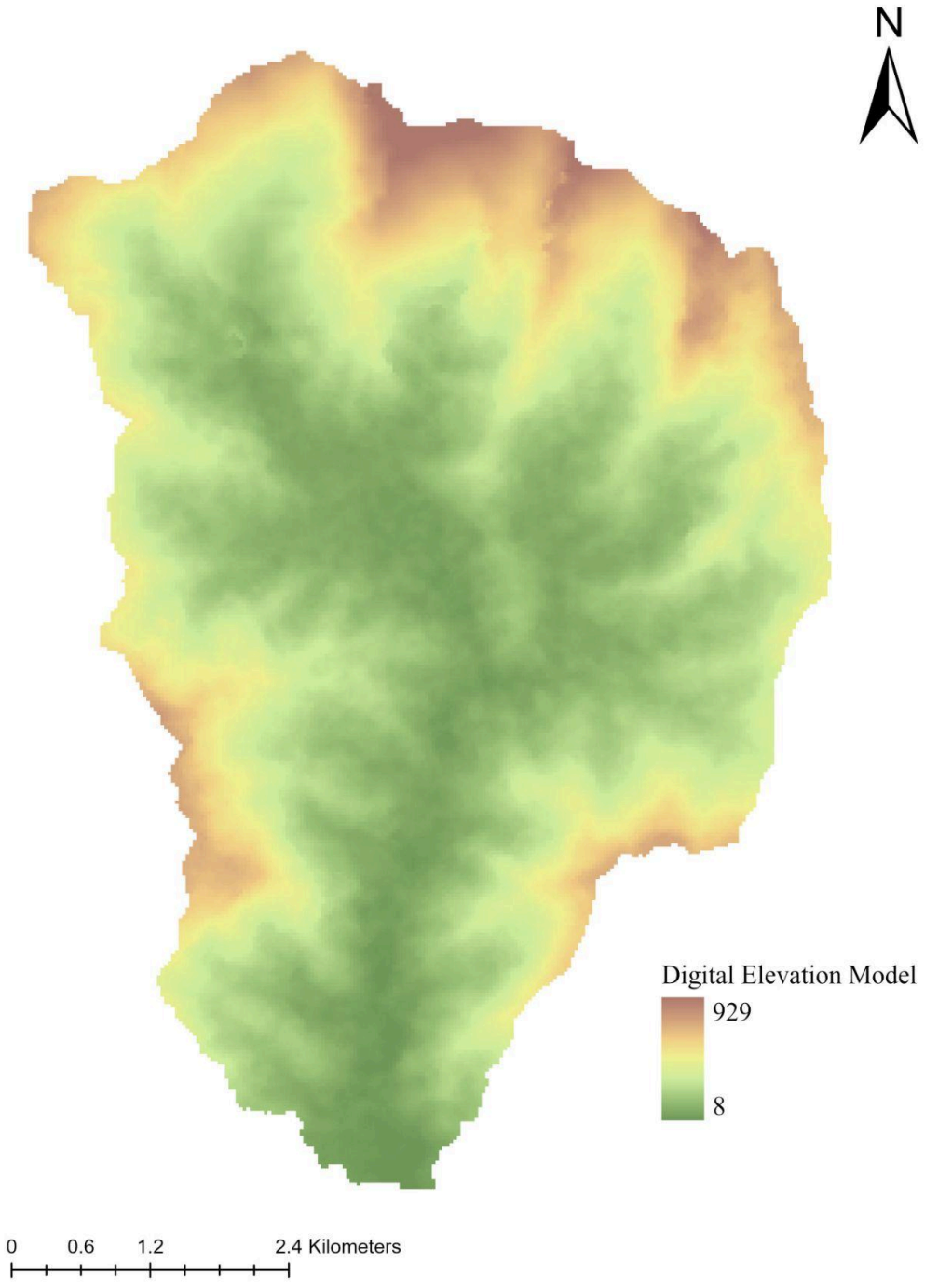

Figure 2. Digital Elevation Model

3.3.2 Rainfall

Due to the lack of data availability from rainfall stations within the catchment, climate data for this study were sourced from historical records provided by the Trinidad and Tobago Meteorological Service at the Piarco rainfall measurement station. An Excel spreadsheet was created to compile the precipitation data for the years 1990, 2000, 2010, and 2020. This data was then used to calculate the rainfall erosivity for each year. While using data from a station outside the immediate study area introduces some uncertainty into the model, it provides a practical approach given the data limitations.

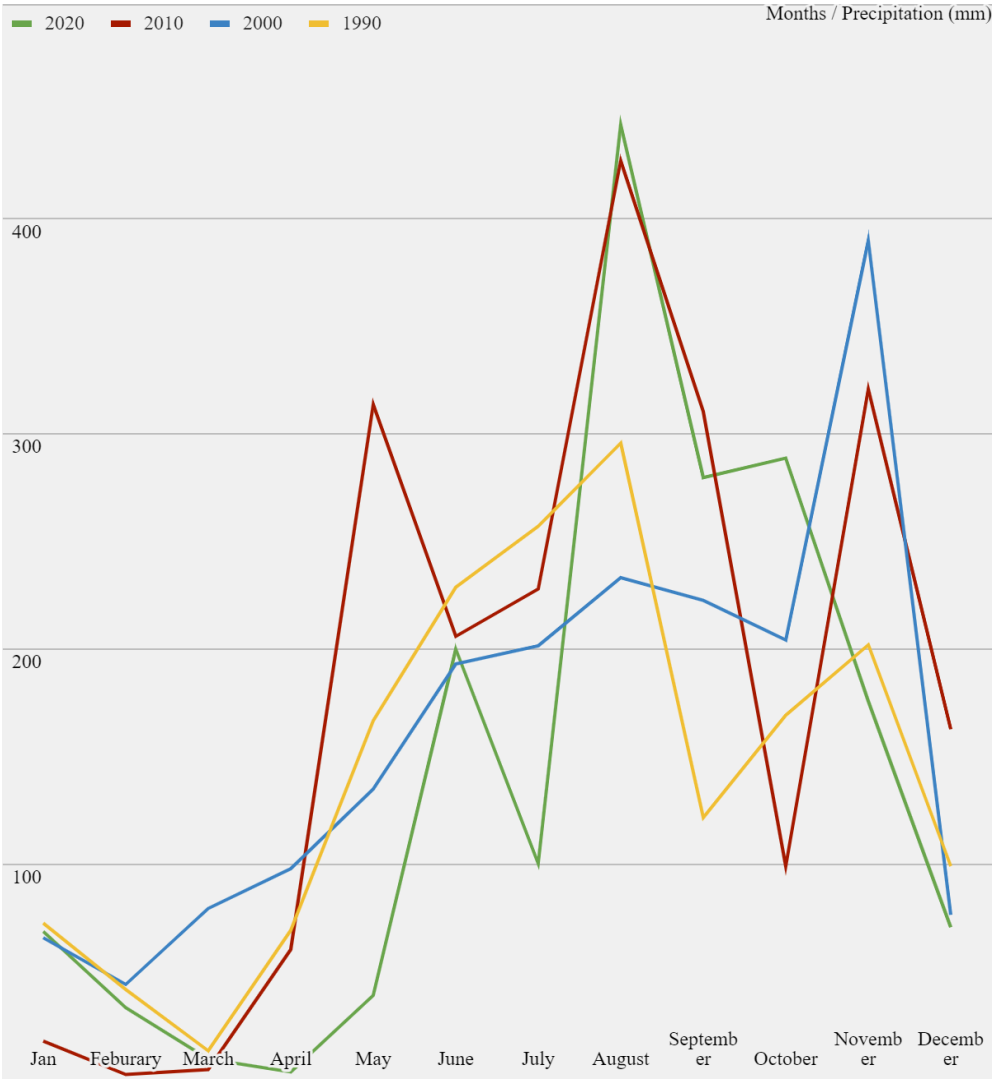

Figure 3. Monthly Precipitation (mm) for 2020, 2010, 2000 and 1990 for Trinidad

3.3.3 Soil Data

The FAO digital soil map of the world (Food and Agriculture Organisation, 2007) was utilised, despite its generalisation of soil types in the area due to limitations in soil data availability for the region. The attribute table of the soil map was examined to identify the soil mapping units present. Each unit had a unique identifier linked to specific soil properties and dominant and associated soils within the study area were determined. Soil properties data from the accompanying supplementary Excel sheet were then used to extract values for percent sand, silt, clay, and organic matter.

3.3.4 Satellite Imagery

Satellite images for the Maracas Valley were sourced and pre-processed within the Google Earth Engine (GEE) platform (Gorelick et al., 2017). The following collections were used:

- Landsat 8 (2013-present): Data for 2020 was retrieved from the `LANDSAT/LC08/C02/T1` collection creating a composite from January to June.
- Landsat 7 (1999-present): Imagery for 2000 and 2010 was obtained from the `LANDSAT/LE07/C02/T1` collection. For 2010, a composite from January to June was created, however, 2000 lacked sufficient data and a composite was created for specific dates: 2000-10-24, 2000-01-29, 2000-08-25, 2000-11-13.
- Landsat 5 (1984-2012): Data for 1990 was retrieved from the `LANDSAT/LT05/C02/T1` collection. 1990 had a similar lack of sufficient data, thus a composite was created for specific dates: 1990-06-08, 1990-09-12, 1990-05-02, 1990-07-21.

Landsat Collection 2 Level 1 products are radiometrically and geometrically corrected to top-of-atmosphere (TOA) reflectance or radiance data. Whereas Landsat Collection 2 Level-2 products are processed and corrected to surface reflectance (SR). Since Level 2 data was not available for the region, Level 1 data was used and atmospherically corrected using dark object subtraction. A cloud and shadow masking function was applied to each image in the collection using the `QA_PIXEL` band. These masks were combined and applied to the images, ensuring that only cloud-free and shadow-free pixels were retained.

Landsat 7 imagery for 2010 contained gaps due to the Scan Line Corrector (SLC) failure. To address this, an additional algorithm was implemented. A focal mean filter with a 1-pixel radius was applied to the images to fill the SLC gaps. The `focal_mean` function was used to calculate the mean pixel value within an 8-pixel neighbourhood, effectively smoothing and filling the gaps. The gap-filled image was then blended with the original Landsat 7 image to produce a seamless final composite. Lastly, a median composite image was generated for each target year using all available cloud-free images within the specified date range.

3.4 RUSLE parameter estimation

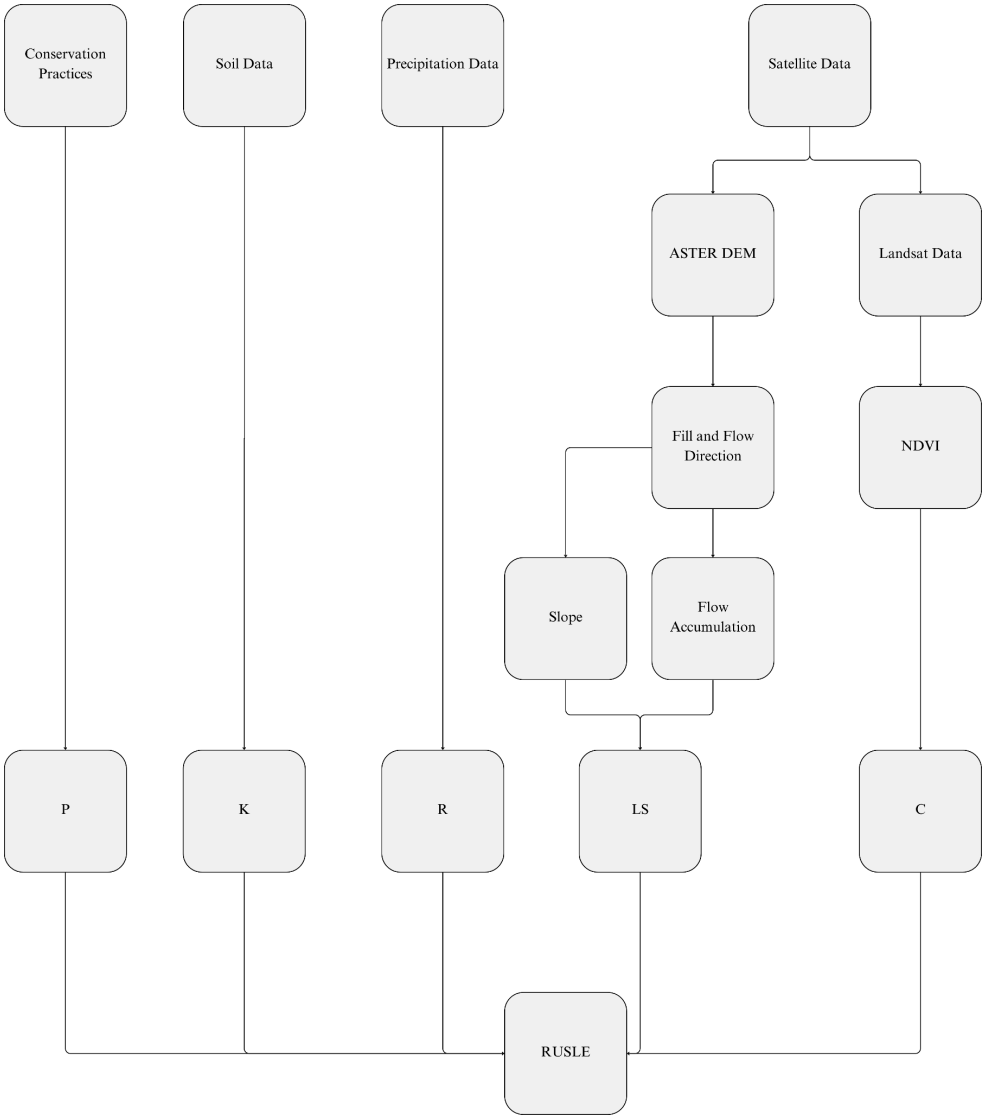

Figure 4. Flowchart of the Methodology

Five parameters are used in the RUSLE model to estimate soil loss. They are rainfall erosivity (*R*), soil erodibility (*K*), slope length and steepness factor (*LS*), cover management factor (*C*) and conservation practice factor (*P*). Referring to RUSLE model, the relationship is expressed as:

$$A = R \times K \times LS \times C \times P$$

Where

- *A* (t ha^{-1} y^{-1}) is the computed spatial average of total soil loss per year
- *R* (MJ mm ha^{-1} h^{-1} yr^{-1}) is the rainfall erosivity factor
- *K* (t ha h ha^{-1} MJ^{-1} mm^{-1}) is the soil erodibility factor
- *LS* is the slope length and steepness factor (dimensionless)
- *C* is the land surface cover management factor (dimensionless)
- *P* is the erosion control or called conservation practice factor (dimensionless).

The methods and formulas for estimating each of the parameters in the model are mainly based on further modifications adapted for tropical environments and data availability.

3.4.1 Rainfall Erosivity

The *R* factor quantifies the impact of rainfall on soil erosion, reflecting the amount and intensity of rainfall events over a specified period (Nearing et al., 2017). In this study, the *R* factor was calculated using precipitation data obtained from the Trinidad and Tobago Meteorological Service. The *R* factor was computed following the methodology outlined by Hurni (1985):

$$R = -8.12 + (0.562 * MAP)$$

Where MAP is the Mean Annual Precipitation (mm).

3.4.2 Soil Erodibility

Soil erodibility values were estimated based on the FAO digital soil map of the world (Food and Agriculture Organisation, 2007), which contains the soil classification according to FAO standards. Soil properties data from the accompanying supplementary Excel sheet were then used to extract values for percent sand, silt, clay, and organic matter. The weighted averages were then derived based on the percentage dominance of each soil type.

Table 1. Soil Composition (%) and Organic Carbon Content (OC) (%)

Soil Unit	Percentage (%)	sand %	silt %	clay %	OC %
Dominant Soil	70	53.6	15.8	30.6	2.25
First Associated Soil	30	58.9	16.2	24.9	0.97
Weighted A		56.25	15.92	28.89	1.866

The dominant soil in the area comprises 70% of the total soil composition, with a sand content of 53.6%, silt content of 15.8%, clay content of 30.6%, and an organic carbon content of 2.25%. The first associated soil unit, making up 30% of the area, has slightly higher sand and silt contents, at 58.9% and 16.2%, respectively but lower clay content at 24.9% and organic carbon content at 0.97%. The weighted averages for the area, which combine these two soil units, result in a soil composition of 56.25% sand, 15.92% silt, 28.89% clay, and 1.866% organic carbon in the topsoil. These values were used to calculate the *K* factor, providing an estimate of the soil's susceptibility to erosion based on its texture and organic matter content. Various methods can be used based on data availability, as the FAO soil map provides the data needed for the method proposed by Williams (1990), the following equation was used:

$$K = (0.2 + 0.3e^{[-0.0256SAN(1-(\frac{SIL}{100}))]}) \times (\frac{SIL}{CLA+SIL})^{0.3} \times (1 - (\frac{0.25c}{(C+e^{(3.72-2.95C)})}) \times (1 - \frac{0.7SN_1}{(C+e^{(3.72-2.95C)}})$$

Where:

- SAN is sand content (%)
- SIL is silt content (%)
- CLAY is clay content (%)
- *C* is soil organic content (%)
- $SN_1 = (1 - SAN/100)$

3.4.3 Slope Length and Steepness

The ASTER GDEM (NASA et al., 2019) was used to derive the necessary topographic parameters for calculating *LS* in the Maracas Valley. The DEM provides elevation data with a spatial resolution of 30 metres. The slope gradient for each cell in the DEM was computed in

degrees using ArcGIS Pro. Flow accumulation, representing the amount of water flow converging at each cell, was calculated using a flow direction algorithm that tracks the movement of water across the landscape (Zhang et al., 2017). The *LS* factor was estimated using the equation proposed by Moore and Burch (1986):

$$LS = (Flow\ accumulation) \times (Cell\ size \times 22.13)^{0..4} \times \left(\frac{\Theta\ slope}{0.0896}\right)^{1.3}$$

Where

- LS is the combination of slope length and steepness
- Flow accumulation is the accumulated upslope contribution to a cell
- Cell size is the resolution of the raster image
- θ slope is the sin value of the slope in degrees

3.4.4 Cover Management and NDVI

In this study, NDVI was calculated using the pre-processed satellite images in GEE using the ee.Image.normalizedDifference function (Gorelick et al., 2017) which calculates NDVI as

$$NDVI = \frac{NIR - RED}{NIR + RED}$$

Where NIR is Near-Infrared band and RED is the red band

After calculating NDVI, the *C* factor can be estimated by applying the relationship used by Durigon et al. (2014) for tropical environments. The equation establishes a direct relationship between NDVI and the *C* factor. Dense vegetation (high NDVI) leads to a lower *C* factor, indicating reduced soil erosion. By rescaling NDVI to a range that effectively and directly links to soil erosion, this method converts a measure of vegetation health into a soil erosion factor that integrates into the RUSLE model.

$$C = 0.1 \times \left(\frac{-NDVI + 1}{2}\right)$$

Due to the persistent cloud cover in tropical environments, the quality of the satellite images may still be affected despite the application of cloud masking algorithms in Google Earth Engine (GEE). While these algorithms significantly reduce cloud-related artefacts, they are not flawless,

which could introduce some uncertainties into the results. These limitations will be further explored in the discussion.

3.4.5 Support Practice Factor

The *P* factor accounts for the effect of soil conservation practices on soil erosion. The P factor ranges from 0 to 1, where lower values indicate more effective conservation practices that reduce soil erosion (Luvai et al., 2022). Available data indicates that there are no significant conservation practices implemented across the Maracas Valley that would influence soil erosion substantially (Jaramillo, 2007; Maracas Valley Action Committee, 2010). Thus, in this study, the *P* factor was assigned a value of 1 for the entire study area. This assignment reflects the lack of significant conservation practices within the Maracas Valley. While conservation practices are present such as reforestation, these practices are minimal and are more likely to influence the *C* factor as opposed to the support practice factor (Jaramillo, 2007).

3.5 Correlation Analysis

To quantify the relationship between vegetation cover and soil erosion in the Maracas Valley, a correlation analysis was conducted between the NDVI values and the soil erosion estimates generated by the RUSLE model. Utilising the rasterio (GDAL, 2024), numpy (Harris et al., 2020) and pandas (The pandas development team, 2024) libraries in python, the NDVI and RUSLE soil erosion values were spatially aligned to ensure that each pixel or spatial unit within the study area had corresponding NDVI and soil erosion values. Spearman's rank correlation coefficient was utilised to assess the strength and direction of the relationship between NDVI and soil erosion for each year. This non-parametric method was chosen due to its ability to capture monotonic relationships without assuming a linear relationship between the variables (Sahoo et al., 2019). The correlation analysis was performed for each year separately, resulting in four sets of correlation coefficients corresponding to the years 1990, 2000, 2010, and 2020. The resulting Spearman's correlation coefficients were used to interpret the relationship between NDVI and soil erosion. A negative correlation would suggest that higher NDVI values are associated with lower soil erosion rates, while a positive correlation would suggest the opposite (Durigon et al., 2014).

3.6 Sensitivity Analysis

To assess the influence of other factors on soil erosion within the RUSLE model, a sensitivity analysis was conducted (Estrada-Carmona et al., 2016). This analysis involved systematically removing each factor from the model calculation to evaluate its relative contribution to the overall soil erosion rates. The factors considered in the sensitivity analysis were rainfall erosivity, soil erodibility, slope length and steepness, cover management and support practice. For each year under study, the RUSLE model was initially run with all factors included to establish a baseline soil erosion rate. Subsequently, each factor was removed one at a time from the model, and the soil erosion rate was recalculated without the removed factor. The resulting changes in soil erosion rates were recorded, providing insights into the sensitivity of the model to each specific factor. The sensitivity of each factor was quantified by comparing the soil erosion values from the full model to those from the modified models with one factor removed.

4. Results

The following section presents the results from the RUSLE parameters and model used to fulfil the aims of this study. Section 4.1 displays results produced from each parameter within the RUSLE model, Section 4.2 displays the output of the RUSLE model from 1990 to 2020 and Sections 4.3 and 4.4 displays the results of the correlation analysis between RUSLE and NDVI as well as the results of the sensitivity analysis between RUSLE and its parameters, respectively.

4.1 Parameters

4.1.1 Rainfall Erosivity

Rainfall erosivity was calculated using historical precipitation data for the Maracas Valley, Trinidad, for the years 1990, 2000, 2010, and 2020. The results reflect the variability in annual precipitation and its corresponding impact on soil erosion across different years where higher *R* values reflect higher erosive power.

Table 2. Annual Precipitation (mm) and Rainfall Erosivity (MJ mm ha^{-1} h^{-1} yr^{-1}) within Maracas Valley, Trinidad.

Year	Annual Precipitation (mm)	*R* (MJ mm ha^{-1} h^{-1} yr^{-1})
1990	1736.3	1123.8576
2000	1942.6	1258.3652
2010	2152.0	1394.8940
2020	1712.3	1108.2096

The results indicate significant variability in the R factor across the different years. The highest R factor was observed in 2010, with a value of 1394.8940 MJ mm ha^{-1} h^{-1} yr^{-1}, corresponding to the highest annual precipitation of 2152.0 mm. This year was characterised by a drought in the early months, which was followed by significant rainfall in the latter part of the year, compensating for the earlier dry season deficit. Thus, contributing to the higher *R* factor. Conversely, the lowest *R* factor was recorded in 2020, with a value of 1108.2096 MJ mm ha^{-1} h^{-1} yr^{-1}, corresponding with the lower annual precipitation of 1712.3 mm.

4.1.2 Slope Length and Steepness

Slope Length and Steepness was calculated using a digital elevation model based on the methodology by Moore & Burch (1986). Figure 5 illustrates the spatial variation of slope length and steepness within the study area, ranging from 0 to 276 with higher values reflecting longer and steeper slopes with greater potential to facilitate soil erosion. In the Maracas Valley, over 90% of slope length and steepness values are below 100. Values of 0 are predominantly observed close to the river's main alluvium areas due to flat land; where the main urbanised areas in the region are concentrated. Conversely, the highest *LS* factor values, reaching up to 276, are found in the more mountainous and steep terrain of the valley.

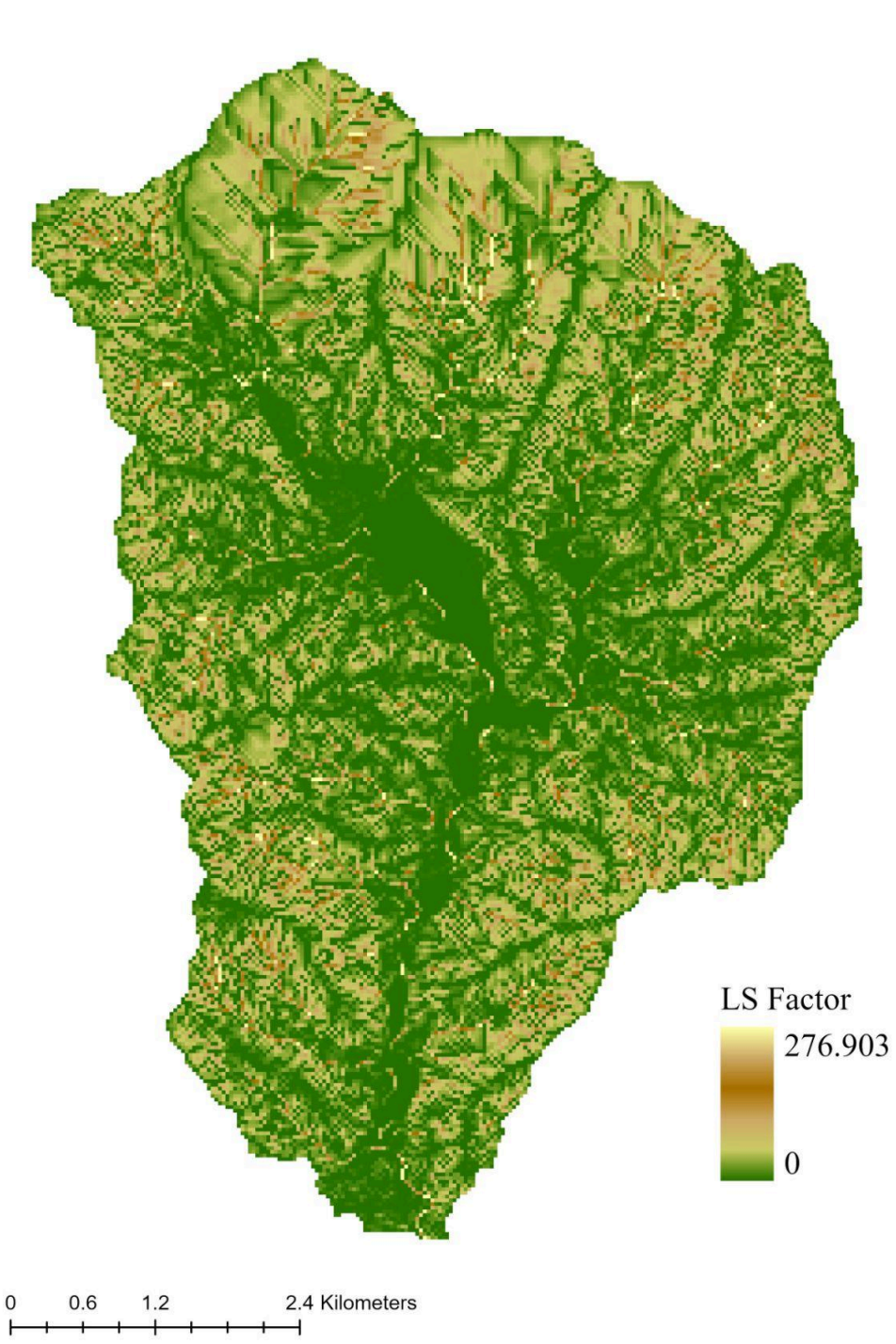

Figure 5. Land Slope and Steepness Factor

4.1.4 Cover Management

Cover Management was calculated using the methodology proposed by Durigon et al. (2014) which rescales the NDVI to a range that effectively maps to erosion with higher *C* factors reflecting increased potential for soil erosion and lower *C* factors reflecting reduced potential for soil erosion. Figures 6 to 9 illustrate the *C* factor for the years 1990 to 2020.

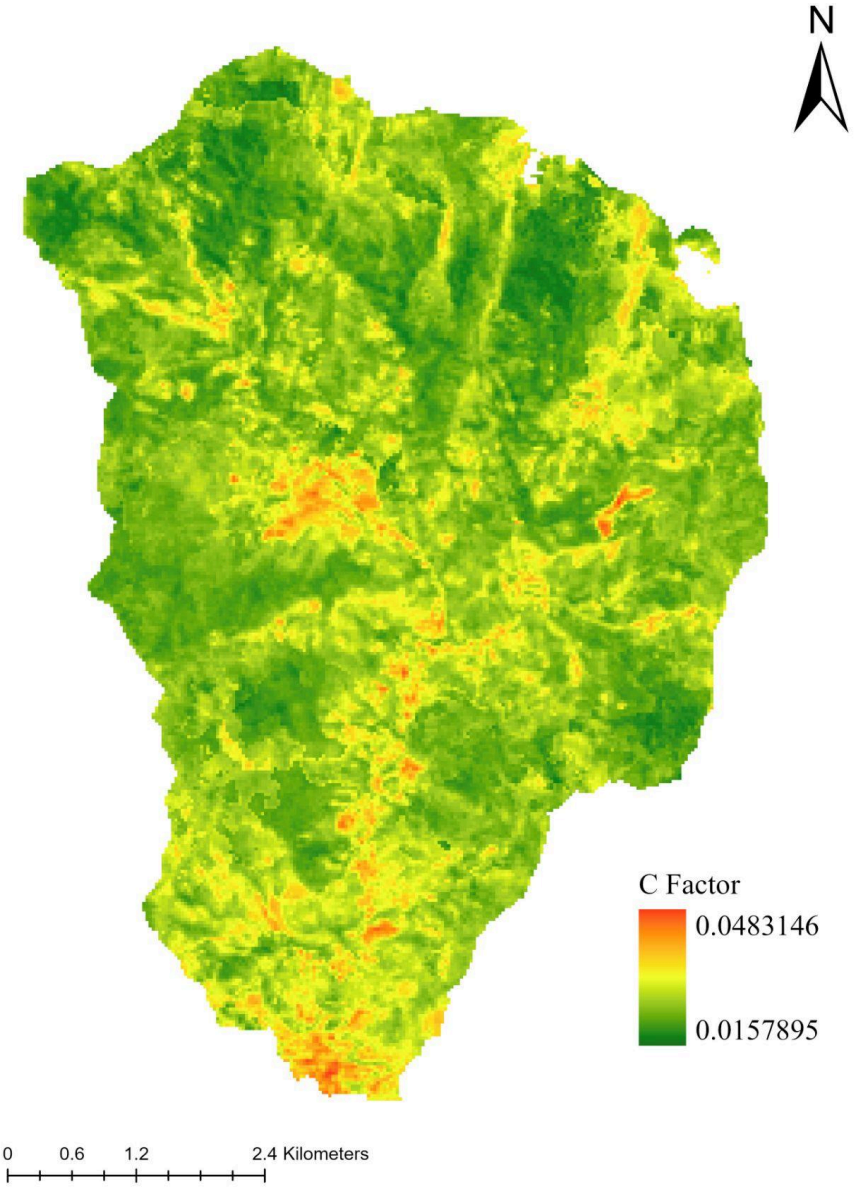

Figure 6. C Factor for 1990

For the year 1990, the *C* factor varies from 0.015 to 0.048 with higher C factors concentrated in

the urbanised areas and along areas of bare land with the highest value at the Coosal Maracas Limestone Quarry to the east of the region. Landsat 5 imagery was used to derive these values; however, due to the limited availability of imagery from 1990, extensive cloud masking was necessary. This process, while essential, resulted in some irregularities in the final output.

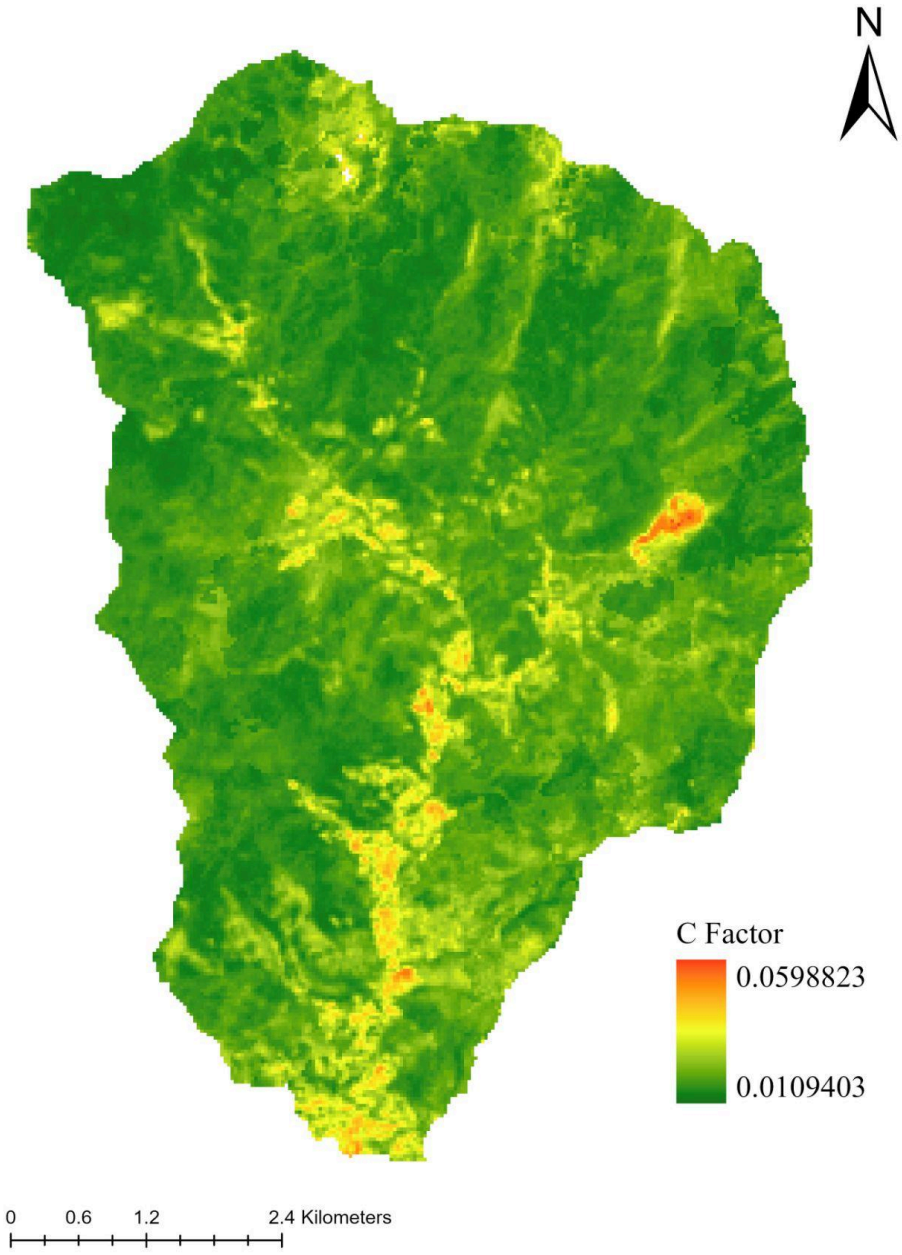

Figure 7. C Factor for 2000

For the year 2000, the *C* factor varies from 0.011 to 0.059. A reduction in land cover along

mountain ridges was observed from 1990 as well as the expansion of the Coosal Maracas Limestone Quarry.

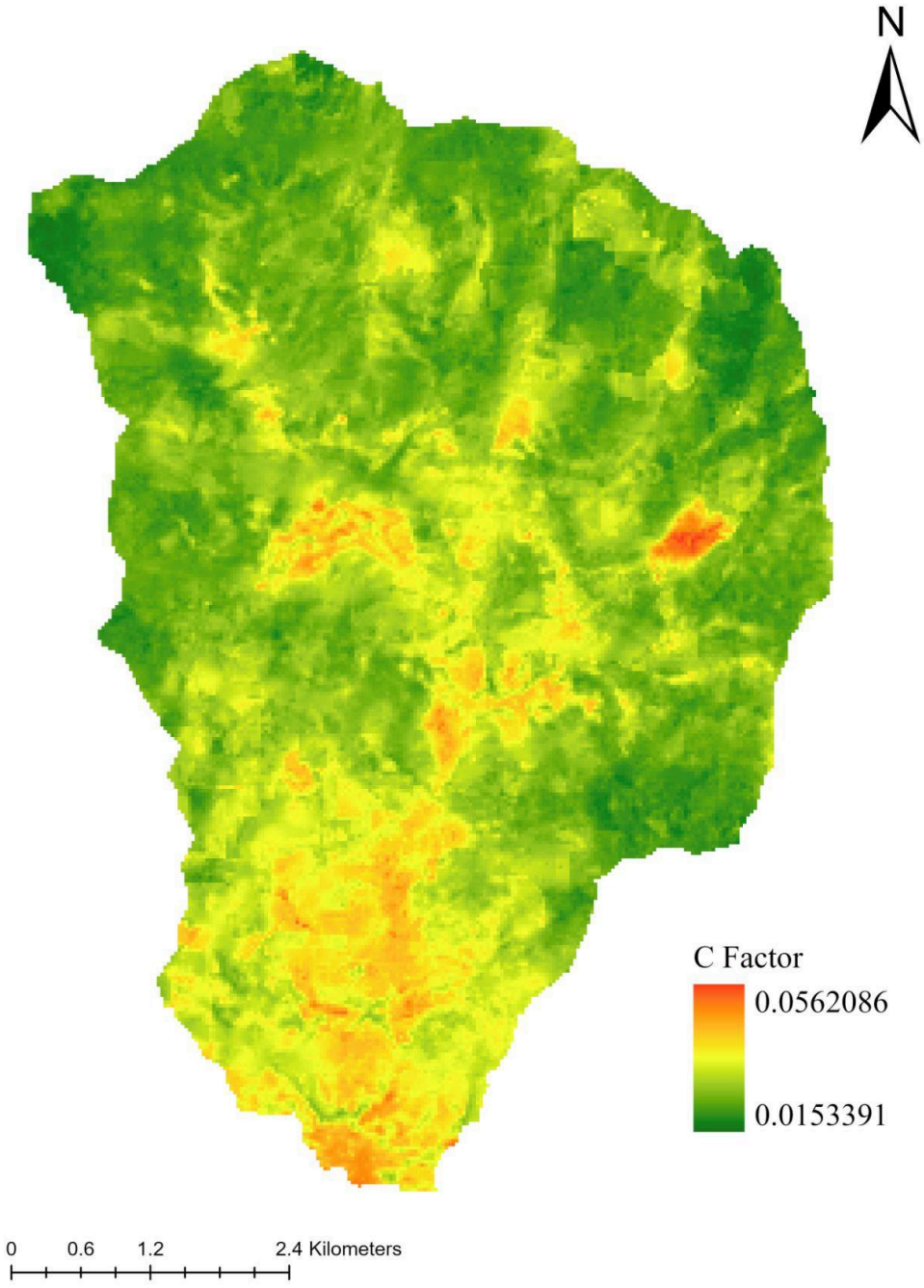

Figure 8. C Factor for 2010

For the year 2010, the *C* factor varies from 0.015 to 0.056. These results reflect the severe

drought with increased bare land along mountain ridges as well as the further expansion of the Coosal Maracas Limestone Quarry from 2000. Due to the Scan Line Error in Landsat 7 from 2003, extensive pre-processing was necessary to fill the resulting gaps in the imagery.

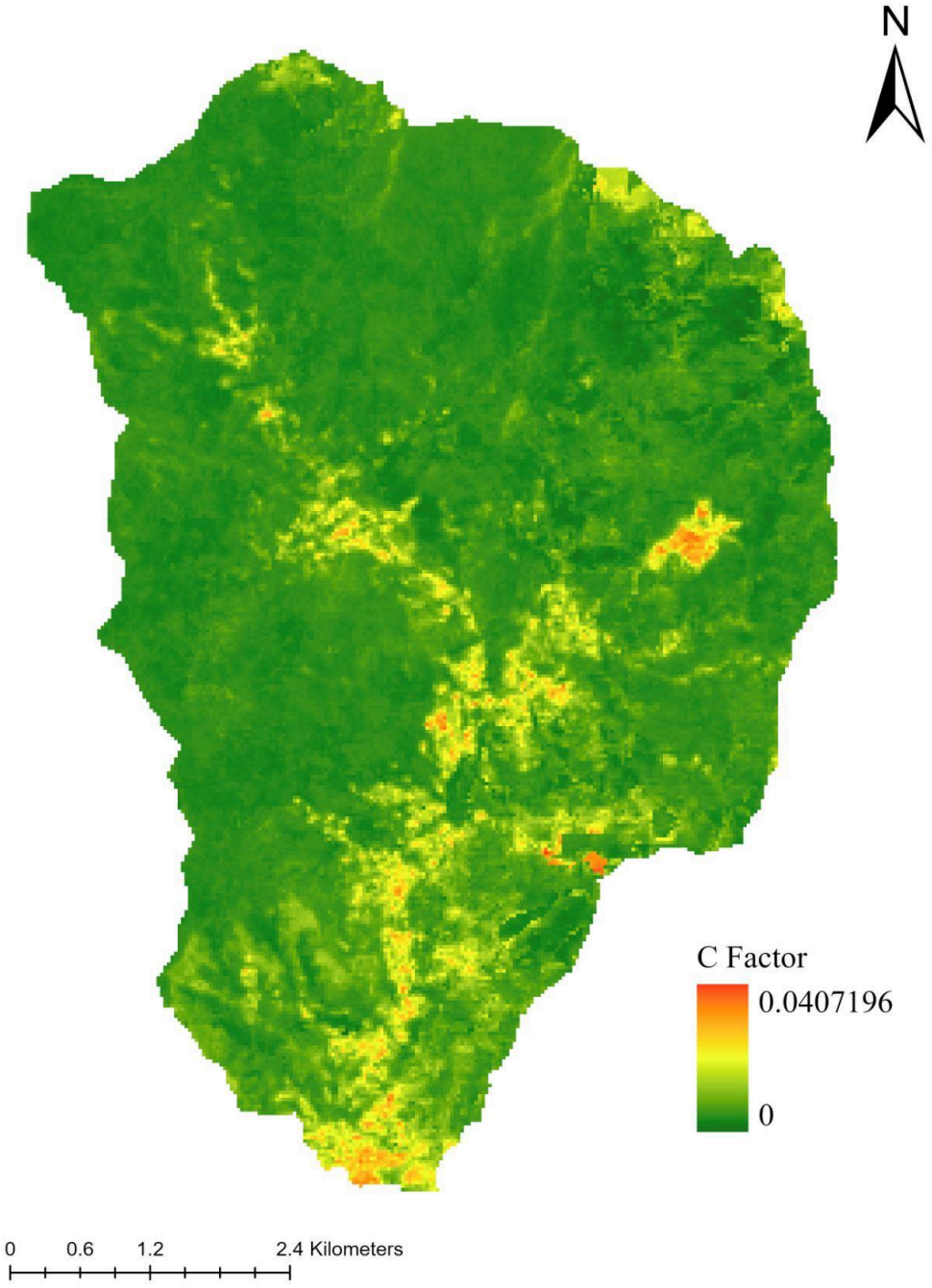

Figure 9. C Factor for 2020

For the year 2000, the *C* factor varies from 0.00 to 0.041 and extensive reforestation was observed from 2010.

4.1.1 Soil Erodibility

The *K* factor typically ranges from 0 to 1, with values closer to 1 indicating soils that are more prone to erosion. The *K* factor for the Maracas Valley was determined to be 0.848, suggesting the soil in this region is highly prone to erosion.

4.1.5 Support Practice

The *P* factor represents the effectiveness of soil and water conservation practices in reducing soil erosion and ranges from 0 to 1, with values closer to 0 indicating more effective conservation practices and a value of 1 indicates no conservation practices. The *P* factor was assigned a value of 1 across the entire Maracas Valley, reflecting the absence of significant conservation practices in the study area. Thus, the model assumes no additional effects from conservation practices on soil erosion in the area.

4.2 RUSLE Model

Soil erosion was calculated based on the formula proposed by Wischmeier and Smith (1978) seen in Table 3 and was reclassified based on the classification system by Sidi Almouctar et al. (2021) seen in Table 4. Figures 10 to 13 illustrate the spatial configuration of soil erosion across the study area for the years 1990 to 2020.

Table 3. Minimum, maximum and mean soil erosion for the years 1990, 2000, 2010 and 2020.

Year	Minimum	Maximum	Mean
1990	0	8850.668	266.885
2000	0	9717.351	224.228
2010	0	12464.693	361.582
2020	0	4781.35	59.491

Table 4. Soil Erosion Classes (Sidi Almouctar et al., 2021).

Erosion Class	Numeric Range (t ha^{-1} y^{-1})
Low	0 - 10
Moderate	10 - 50
High	50 - 150
Very High	150 - 200
Severe	> 500

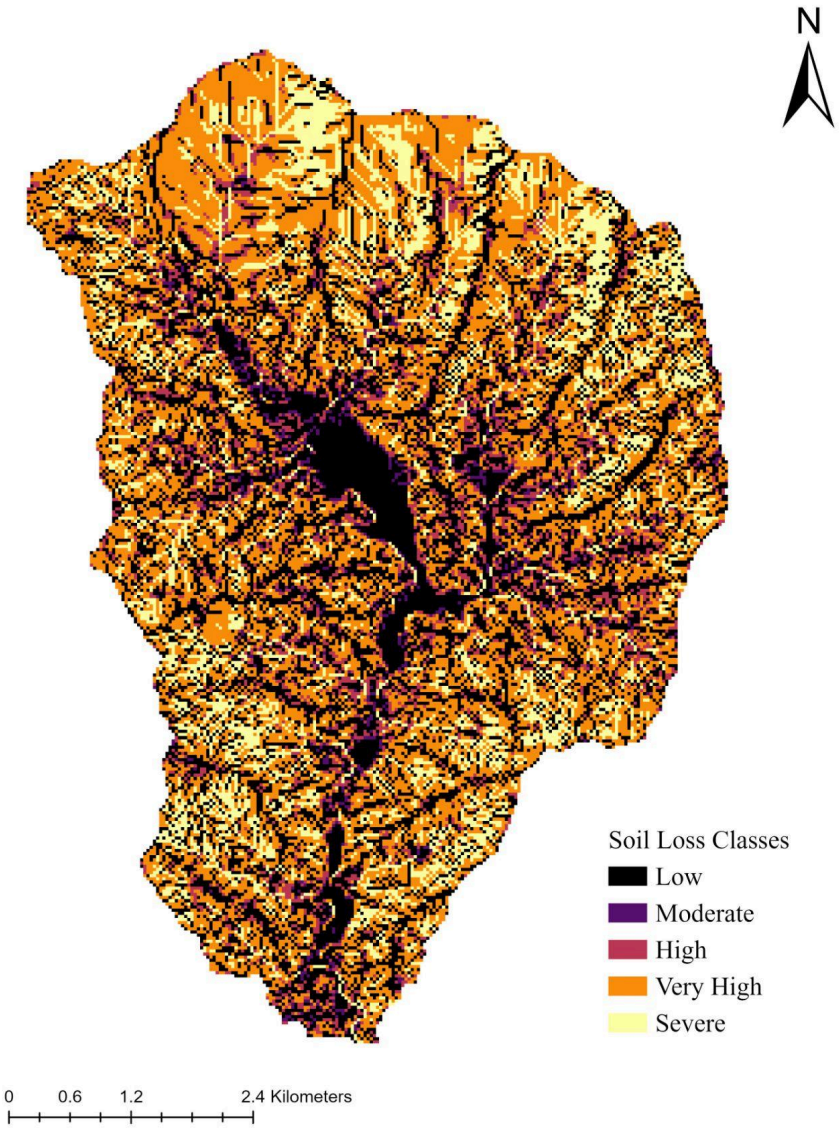

Figure 10. RUSLE model for 1990

In 1990, the mean soil erosion was 266.885 t ha^{-1} y^{-1}, with values ranging from 0 to 8850.668 t ha^{-1} y^{-1}. 34.36% of the study area falls within the low erosion category. The moderate category accounts for 1.76% of the area, while 8.54% of the area is classified as high soil erosion. The majority of the region experiences very high and severe soil erosion at 38.63% and 16.70% respectively.

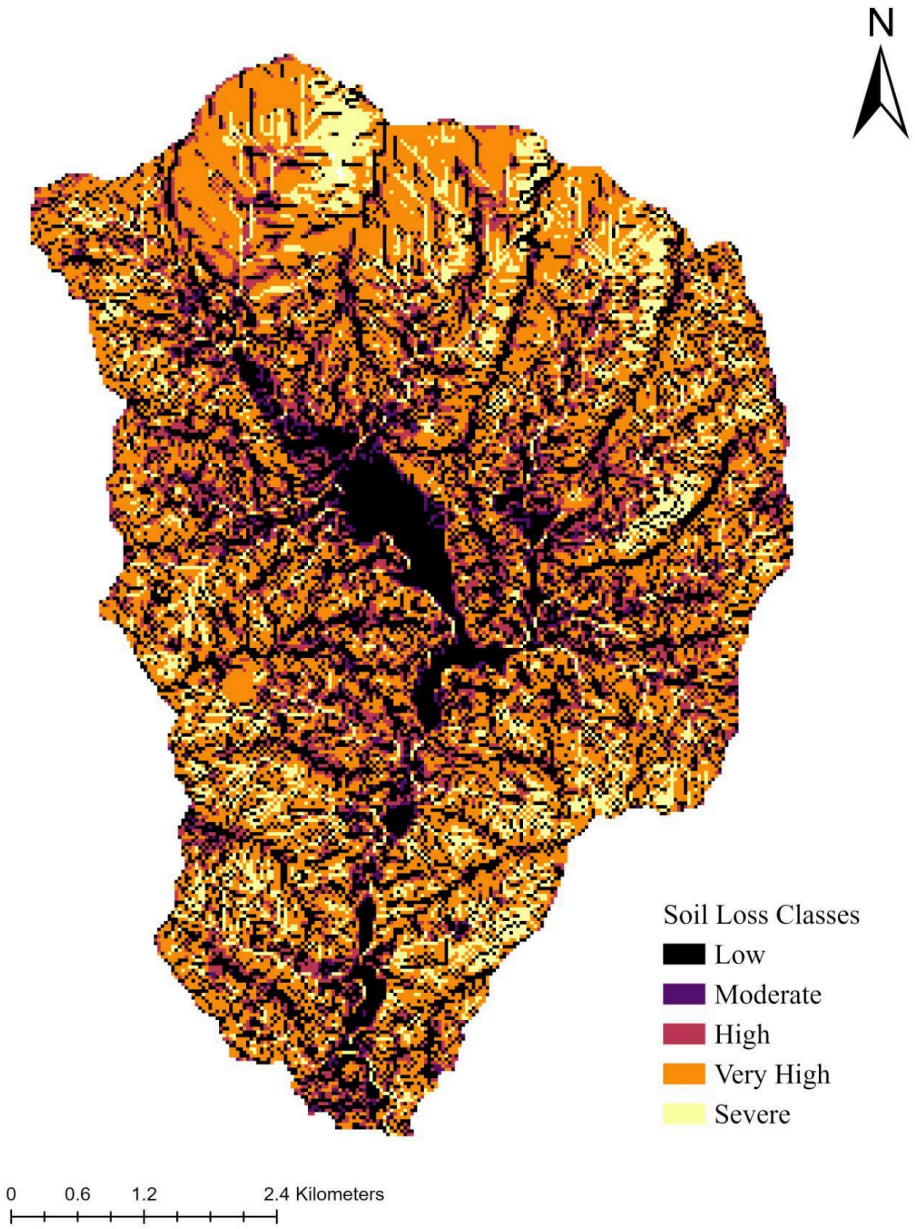

Figure 11. RUSLE model for 2000

The year 2000 had a mean erosion of 224.228 t ha^{-1} y^{-1}, with a range from 0 to 9,717.351 t ha^{-1} y^{-1}. Similar to 1990, 34.40% of the study area falls within the low erosion category. The moderate category accounts for 2.09% of the area, while 12.62% of the area is classified as high soil erosion. The majority of the region experiences very high and severe soil erosion at 39.15% and 11.72% respectively. However, these categories decreased by 4.5% since 1990.

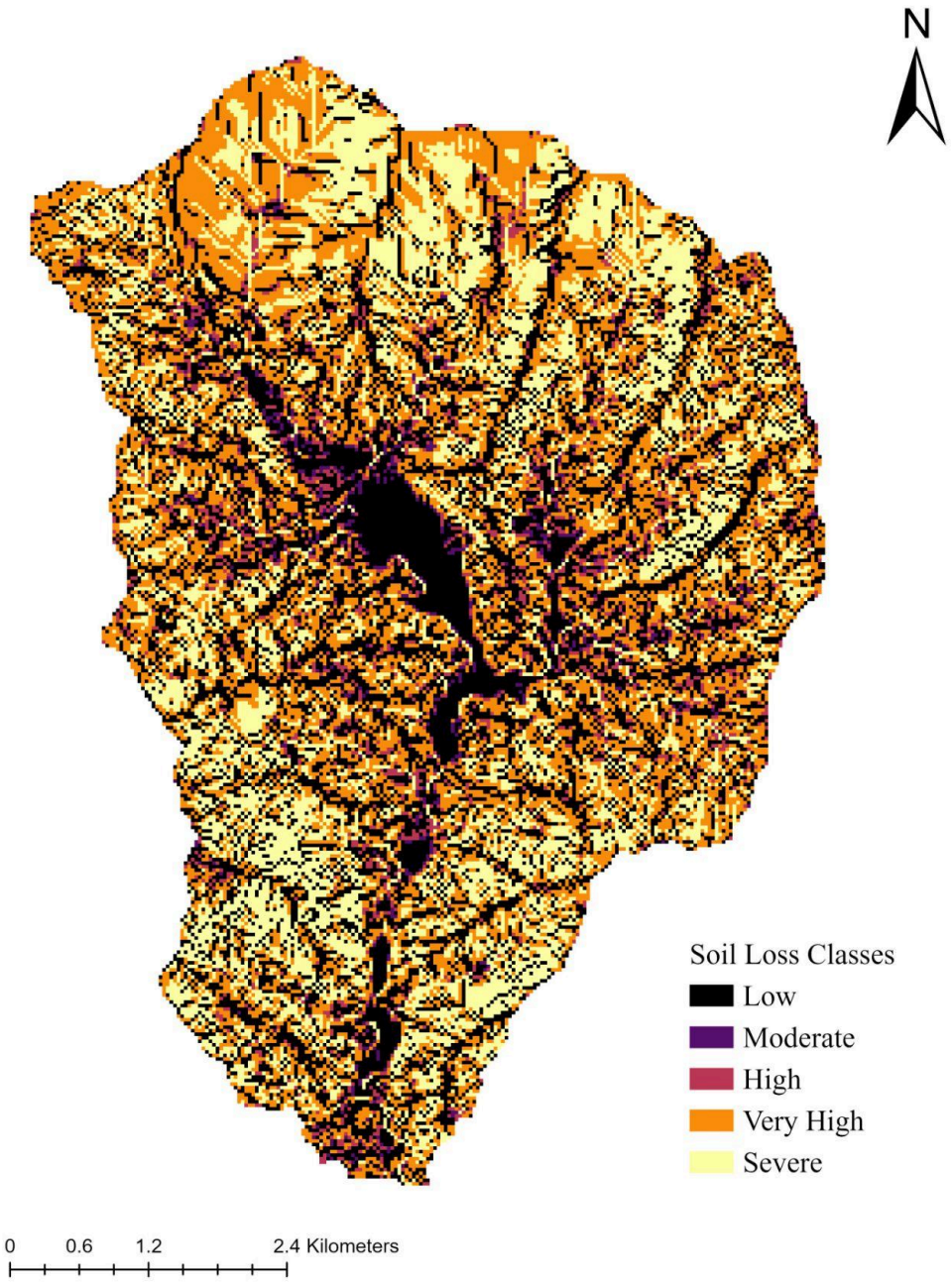

Figure 12. RUSLE model for 2010

In 2010, the mean erosion significantly increased to 361.582 t ha^{-1} y^{-1}, with values ranging from 0 to 12,464.693 t ha^{-1} y^{-1}. 34.19% of the study area falls within the low erosion category. The moderate category accounts for 1.29% of the area, while 4.94% of the area is classified as high soil erosion. The majority of the region experiences very high and severe soil erosion at 33.05% and 26.52% respectively with the severe category increasing by 14.80% since 2000.

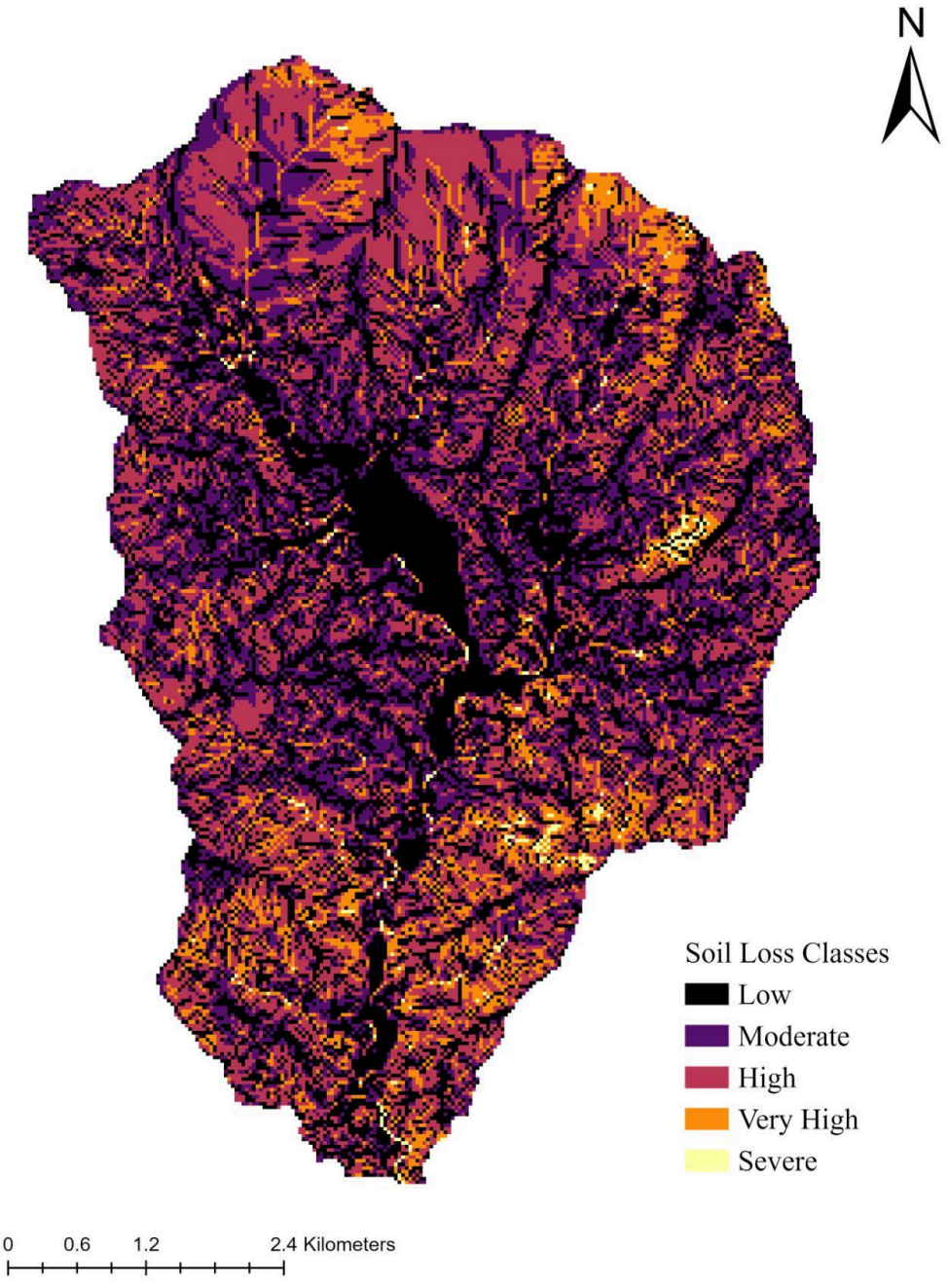

Figure 13. RUSLE model for 2020

In 2020, the mean erosion value decreased significantly to 59.491 t ha^{-1} y^{-1}, with a range from 0 to 4,781.35 t ha^{-1} y^{-1}. The majority of the study area, 36.25%, now falls within the low erosion category. The moderate category accounts for 24.13% of the area, while 30.44% of the area is classified as high soil erosion. Classes of very high and severe soil erosion significantly decreased to 8.49% and 0.69%, respectively.

4.3 Correlation Analysis

Table 5. Spearman's Correlation Coefficients Between NDVI and Soil Erosion for 1990 to 2020.

Year	Spearman's Correlation (NDVI, Soil Erosion)
1990	0.083
2000	0.064
2010	0.080
2020	-0.015

From table 5, the years 1990, 2000, 2010, and 2020 all show very weak correlation between NDVI and soil erosion. The years 1990, 2000 and 2010, all suggest a very weak positive correlation at 0.083, 0.064 and 0.080 respectively while 2020 shows a very weak negative correlation and -0.015.

4.4 Sensitivity Analysis

The sensitivity analysis for the years 1990, 2000, 2010 and 2020 was used to determine the impact of removing individual RUSLE factors on soil erosion estimates; assessing its relative influence on the predicted soil erosion rates. Thus, providing insight into the factors that are most critical for accurate soil erosion modelling and identifying key variables that drive soil erosion in the Maracas Valley.

Table 6. Sensitivity Analysis

Year	Description	Minimum	Maximum	Mean	Standard Deviation
1990	Removal of R	0	7.875	0.237	0.312
	Removal of K	0	10437.108	314.723	413.232
	Removal of LS	15.048	46.045	24.806	4.298
	Removal of C	0	263897.593	10567.656	13590.227
	Removal of P	0	8850.668	266.885	350.421
	RUSLE	0	8850.668	266.885	350.421
2000	Removal of R	0	7.722	0.178	0.246
	Removal of K	0	11459.14	264.420	364.965
	Removal of LS	11.674	63.900	21.153	5.923
	Removal of C	0	295481.90	11832.435	15216.758
	Removal of P	0	9717.351	224.228	309.490
	RUSLE	0	9717.351	224.228	309.490
2010	Removal of R	0	8.93	0.259	0.346
	Removal of K	0	14698.93	426.39	568.868
	Removal of LS	18.144	66.487	33.918	7.505
	Removal of C	0	327540.781	13116.218	16867.730
	Removal of P	0	12464.693	361.582	481.401
	RUSLE	0	12464.693	361.582	481.401
2020	Removal of R	0	4.314	0.053	0.096
	Removal of K	0	5638.39	70.155	125.544
	Removal of LS	0	38.269	5.900	4.140
	Removal of C	0	260223	10420.518	13401.003
	Removal of P	0	4781.35	59.491	106.460
	RUSLE	0	4781.35	59.491	106.460

In 1990, removing the *R* factor decreased the mean erosion rate to 0.237 t ha^{-1} y^{-1} ± 0.312 indicating a moderate impact with minimal variability. This pattern remained consistent in the following years, reducing the mean erosion rate significantly to 0.178 t ha^{-1} y^{-1} in 2000, 0.259 t ha^{-1} y^{-1} in 2010 and 0.053 t ha^{-1} y^{-1} in 2020. Removing the *K* factor increased the mean erosion rate significantly to 314.723 t ha^{-1} y^{-1}, with a standard deviation of 413.232 in 1990, indicating high variability. Similar substantial increases were observed in 2000, 2010, and 2020, suggesting that the *K* factor has a significant and consistent influence on soil erosion rates in the Maracas Valley.

For the *C* factor, removing it in 1990 caused a significant increase in mean erosion rate to 10,567.656 t ha^{-1} y^{-1} with a standard deviation of 13,590.227 indicating high variability. This trend was also evident in the following years where removing the *C* factor led to substantial increases in soil erosion rates, indicating that the *C* factor has a major effect on the model. For the *LS* factor, removing it in 1990 reduced the mean erosion rate to 24.806 t ha^{-1} y^{-1} with a standard deviation of 4.298. This reduction was consistent across all years, showing that while the *LS* factor has an influence, it is not as substantial as the *K* or *C* factors. Lastly, removing the *P* factor had no effect on the mean erosion rate or standard deviation for any of the years in the study period, highlighting its negligible impact on soil erosion in this context

5. Discussion

5.1 Spatial and Temporal Trends in Soil Erosion

RUSLE is an empirical-based modelling approach that predicts the long-term average annual rate of soil erosion on slopes (Renard et al., 1997). The spatiotemporal dynamics of soil erosion in the Maracas Valley, Trinidad and Tobago, have been closely examined using the RUSLE model along with NDVI data, which provides valuable insight into how land cover changes have influenced erosion rates over the past several decades.

The temporal trends in soil erosion from 1990 to 2020 indicate a notable shift towards lower erosion over time. In 1990, 55% of the area was classified under Very High and Severe categories. However, by 2020, these high soil erosion categories significantly decreased to 9%.

Despite this, 30% of the area still remained in the high category. The 2010 spike in soil erosion can be accounted for by the severe drought and forest fires that affected the Caribbean from 2009 to 2010, significantly reducing vegetative cover in the Northern Range (Peters, 2015). Figure 2 demonstrates the negligible precipitation in the first quarter of 2010, increasing sharply at the onset of the rainy season. The high R factor 1394.8940, illustrates this phenomenon, where the impact of a severe drought in the dry season was compounded by subsequent heavy rainfall in the wet season.

The sudden increase in rainfall intensity on slopes with compromised vegetation, can result in significant runoff, leading to the spike in soil erosion at 361.582 t ha^{-1} y^{-1}. The initiatives of the NRWRP have been instrumental in managing these challenges as by the 2009 forest fires, extensive fire traces had been established to create a barrier preventing the fires from reaching and damaging the 70 acres of reforested land established through the programme (Maracas Valley Action Committee, 2010). Thereby, allowing for further reforestation and retention of reforested areas by 2020.

While methodologies for estimating the *R* factor can vary, potentially leading to discrepancies in reported values, the findings for the Maracas Valley are consistent with those from studies utilising similar approaches in regions with comparable annual precipitation. For instance, Andriyani et al. (2024) estimated a maximum rainfall erosivity of 1241.86 MJ mm ha^{-1} h^{-1} $year^{-1}$ in the Mayang Watershed, Indonesia, using a similar methodology. However, discrepancies arise when comparing the findings to studies conducted in regions with comparable annual precipitation but utilising different methodologies. For instance, Rodrigues et al. (2017) yielded a result of 8953 MJ mm ha^{-1} h^{-1} $year^{-1}$ in the Brazilian Cerrado. Despite these differences, the consistency of our results with similar studies indicates that the *R* factor is a reliable estimate for the Maracas Valley, reflecting the regional climate conditions and data used.

In over 90% of the study area, *LS* factor values are below 100, indicating that the majority of regions experience relatively low to moderate erosion potential due to topographic conditions. Values of 0 are predominantly observed in flat land close to the river's main alluvium. These flat areas coincide with the primary urbanised regions of the study area. Thus, despite the high level of urbanisation in these regions, soil erosion remains low due to the flat topography. The *K* factor for the Maracas Valley, reflecting the soil erodibility based on texture and organic carbon

content, was calculated to be 0.848. This value is influenced by the dominant soil properties in the area with a weighted average of 56.25% sand, 15.92% silt, 28.89% clay, and 1.866% organic carbon for the combined soil units. Studies with similar percentages of sand, silt, and clay show *K* factors within a similar range of 0.6 to 0.9 (Ghosal and Das Bhattacharya, 2020).

5.2 Factors Influencing Soil Erosion

The Normalised Differential Vegetation Index is an indicator of vegetation health and density based on red and near-infrared reflectance; allowing for efficient identification of vegetated areas (Xue and Su, 2017). In the context of this study, this principle functions as a classification of land cover, distinguishing between vegetated and non-vegetated surfaces. Interestingly, correlation between NDVI and soil erosion across the years show no significant relationship. This may suggest that other factors, such as topography, land management or climate are more dominant in influencing soil erosion in the Maracas Valley. Thus, it is necessary to examine the effects of other factors within the RUSLE model to gain a more comprehensive understanding of soil erosion dynamics.

Model sensitivity analyses are a useful tool in the assessment of model application and the identification of the most influential input parameters (Enrico Balugani et al., 2020). Removing the *C* factor consistently led to dramatic increases in mean erosion rates. Without this factor, the model fails to account for the erosion control mechanisms of vegetation cover, resulting in largely overestimated erosion values with large variability. The weak direct correlation between NDVI and soil erosion may be due to the complex and indirect influence of NDVI, which operates through the *C* factor rather than as a direct determinant. Removing the *K* factor also resulted in notable increases to mean erosion rate. Omitting this factor negates the impact of soil texture and organic content in stabilising slopes; overestimating the amount of soil erosion in the region.

Removal of the *LS* factor resulted in slight decreases in mean erosion rates in the model. Although the changes in mean erosion rates were less dramatic compared to the *C* and *K* factors, the consistent reduction across years indicates that slope length and steepness still plays a notable role. Removing the *R* factor led to a significant decrease in mean erosion rates with low

variability. In the absence of rainfall erosivity, the other factors are not sufficient to maintain high erosion rates as the model predicts minimal erosion. Lastly, the *P* factor did not contribute to significant changes in mean erosion rates. This is expected as the *P* factor was set to 1 in the study.

5.3 Implications for Soil and Water Conservation

Soil erosion has a direct impact on water quality and quantity as sediment from eroded soils can lead to sedimentation in water bodies, adversely affecting aquatic ecosystems and increasing the cost of water treatment (Fontes De Maria and Phillips, 2019). In 2009, the MVAC reported extensive reduction in water supply, higher peak river flows in the rainy season, and frequent flooding due to sedimentation in the Maracas-St. Joseph River (Maracas Valley Action Committee, 2010).

The observed decrease in soil erosion over time illustrates the effectiveness of conservation practices in the Maracas Valley. This reduction implies that conservation practices, such as reforestation and improved soil management, have been effective in stabilising soil and reducing erosion rates. Although this analysis shows a reduction in soil erosion, updated reports from the MVAC are not yet available to provide a current assessment of the efficacy of these practices on soil and water stability.

Given that cover management and soil erodibility are the most significant factors that influence soil erosion in the Maracas Valley, important consideration must be given to prioritising these elements. The conclusion of the National Reforestation and Watershed Rehabilitation Programme in 2014, leaves a gap in ongoing conservation efforts. Thus, it is essential to expand reforestation efforts in regions still experiencing high erosion rates. Reforestation not only helps stabilise soil but also increases watershed health by improving water retention and reducing runoff (Veldkamp et al., 2020).

The presence of the quarry in the Maracas Valley poses a substantial threat to soil and water conservation efforts. As the Maracas River is an important source of water for Trinidad and Tobago, MVAC continues to lobby for the closure of the currently operating quarry and ban on

further quarrying in the watershed. It is also recommended that land previously used for quarrying to be rehabilitated.

Additionally, soil erosion is exacerbated by the practice of unregulated slash and burn agriculture by residents. This method involves clearing land by cutting and burning vegetation as preparation for cultivation. The removal of vegetation and the exposure of bare soil greatly increase the susceptibility of the land to erosion, as the protective cover that stabilises the soil is lost (Kleinman, 1995). The frequent use of this technique without proper land management practices leads to soil degradation, where the soil decreases in fertility and becomes more susceptible to erosion over time.

The Revised Universal Soil Loss Equation can therefore offer actionable insights to inform land use planning, conservation strategies, and soil management practices. It can be used to support the development of targeted erosion control measures and to evaluate the effectiveness of existing policies and guide adjustments to enhance soil conservation efforts. Addressing soil erodibility through further community education and improved soil management such as implementing cover crops and vegetative buffers as well as terracing and contour farming on slopes (Saggau et al., 2023; Ricci et al., 2020) and adopting best management practices such as gully stabilisation and conservation tillage (Seitz et al., 2018) will enhance soil stability.

5.4 Limitations and Future Research

This study presents several limitations that could influence the results and interpretations of soil erosion dynamics in the Maracas Valley. Firstly, in cases where cloud masking is incomplete or inaccurate, residual cloud pixels or shadows can lead to inaccurate NDVI readings. Additionally, while NDVI provides valuable insights into vegetation health, it may not fully capture the range of variability in vegetation types and their effectiveness in preventing soil erosion. Variations in land management practices and specific types of vegetation cover are not always accurately reflected by NDVI values, potentially leading to an underrepresentation of the impact that different vegetation types and management practices have on soil erosion.

Another limitation stems from the use of rainfall data sourced from the Piarco station, provided by the Trinidad and Tobago Meteorological Service, due to the lack of local rainfall data within

the Maracas Valley catchment. This limitation could introduce inaccuracies in the precipitation data used for the RUSLE model, as the rainfall patterns at Piarco may not fully represent those within the Maracas Valley. The study also utilised the FAO digital soil map of the world, which provides generalised descriptions of soil types in the area. This generalisation might oversimplify the variability in soil properties across the catchment, potentially affecting the accuracy of the *K* factor in the RUSLE model and, consequently, the overall erosion values.

Future research should focus on obtaining localised climate data for more accurate erosion modelling, refining soil type classifications, and addressing limitations in data processing. Detailed soil surveys can aid in obtaining soil type classifications that reflect the landscape and would enhance the accuracy of the *K* factor. Additionally, exploring advanced cloud masking techniques and improved satellite imagery could reduce errors in vegetation data, further enhancing the reliability of NDVI calculations.

Additionally, due to the dual nature of Trinidad and Tobago's climate, erosion rates may vary significantly depending on the time of year. Accurately assessing soil erosion in Trinidad, therefore, requires an approach that accounts for the seasonal variations in climate, with targeted strategies for managing erosion during both the dry and wet seasons.

6. Conclusion

This study aimed to investigate the impact of land cover changes on soil erosion in the Maracas Valley and to explore the spatial patterns of soil erosion and factors affecting erosion rates. The analysis revealed that soil erosion in the Maracas Valley has declined considerably from 1990 to 2020. However, the data also highlighted a significant spike in soil erosion in 2010, attributed to a severe drought that affected the region. The correlation analysis between NDVI and soil erosion showed generally weak relationships across the years studied. Spearman's correlation coefficients were very low, indicating minimal direct association between NDVI values and soil erosion rates. These values suggest that while NDVI reflects vegetation cover, its influence on soil erosion in the region, as captured in this study, is negligible. However, the sensitivity analysis revealed that the *C* factor, which incorporates vegetation cover, had a substantial impact on erosion values, emphasising the role of land management practices in erosion control. Other

factors, such as soil erodibility and topography also significantly influenced erosion rates, though their impacts varied by year. The observed reduction in erosion over time, likely influenced by community led conservation initiatives such as those by the Maracas Valley Action Committee, emphasises the importance of effective land management and reforestation efforts. Further studies should aim to obtain more detailed and localised data on soil properties and rainfall.

References

Aburas, M.M., Abdullah, S.H., Ramli, M.F. and Ash'aari, Z.H. 2015. Measuring Land Cover Change in Seremban, Malaysia Using NDVI Index. *Procedia Environmental Sciences*. **30**, pp.238–243.

Amsalu, T. and Mengaw, A. 2014. GIS Based Soil Loss Estimation Using RUSLE Model: The Case of Jabi Tehinan Woreda, ANRS, Ethiopia. *Natural Resources*. **05**(11), pp.616–626.

Andriyani, I., Indarto, I., Soekarno, S. and Pradana, M.P. 2024. Analysis of rainfall erosivity factor (R) on prediction of erosion yield using USLE and RUSLE Model's; A case study in Mayang Watershed, Jember Regency, Indonesia. *Sains Tanah - Journal of Soil Science and Agroclimatology*. **21**(1), pp.64–64.

Arnoldus, H. 1980. An Approximation of the Rainfall Factor in the Universal Soil Loss Equation. In De Boodt, M. and Gabriels, D., Eds., Assessment of Erosion, John Wiley and Sons, New York, 127-132. - References - Scientific Research Publishing. *www.scirp.org*. [Online]. [Accessed 19 July 2024]. Available from: https://www.scirp.org/reference/ReferencesPapers?ReferenceID=1687726.

Babalwa Kafu-Quvane and Sanelisiwe Mlaba 2024. Assessing the Impact of Quarrying as an Environmental Ethic Crisis: A Case Study of Limestone Mining in a Rural Community. *International journal of environmental research and public health/International journal of environmental research and public health*. **21**(4), pp.458–458.

Borrelli, P., Alewell, C., Alvarez, P., Anache, J.A.A., Baartman, J., Ballabio, C., Bezak, N., Biddoccu, M., Cerdà, A., Chalise, D., Chen, S., Chen, W., De Girolamo, A.M., Gessesse, G.D., Deumlich, D., Diodato, N., Efthimiou, N., Erpul, G., Fiener, P. and Freppaz, M. 2021. Soil erosion modelling: A global review and statistical analysis. *Science of The Total Environment*. **780**, p.146494.

Dangler, E.W. and El‐Swaify, S.A. 1976. Erosion of Selected Hawaii Soils By Simulated Rainfall. *Soil Science Society of America journal*. **40**(5), pp.769–773.

Darbayeva, T., Ramazanova, N., Chashina, B., Berdenov, Zh., Mendybayev, E., Wendt, J.A. and Atasoy, E. 2020. Modeling soil erosion in the Chagan river basin of the west Kazakhstan with using RUSLE and GIS tools. *Journal of Environmental Biology*. **41**(2(SI)), pp.396–404.

Darwish, T., Khater, C., Jomaa, I., Stehouwer, R., Shaban, A. and Hamzé, M. 2010. Environmental impact of quarries on natural resources in Lebanon. *Land Degradation & Development*. **22**(3), pp.345–358.

De Jong, S.M. 1994. Derivation of vegetative variables from a landsat tm image for modelling soil erosion. *Earth Surface Processes and Landforms*. **19**(2), pp.165–178.

Defries, R.S. and Townshend, J.R.G. 1994. NDVI-derived land cover classifications at a global scale. *International Journal of Remote Sensing*. **15**(17), pp.3567–3586.

Durigon, V.L., Carvalho, D.F., Antunes, M.A.H., Oliveira, P.T.S. and Fernandes, M.M. 2014. NDVI time series for monitoring RUSLE cover management factor in a tropical watershed. *International Journal of Remote Sensing*. **35**(2), pp.441–453.

Ejaz, N., Elhag, M., Bahrawi, J., Zhang, L., Gabriel, H.F. and Rahman, K.U. 2023. Soil Erosion Modelling and Accumulation Using RUSLE and Remote Sensing Techniques: Case Study Wadi Baysh, Kingdom of Saudi Arabia. *Sustainability*. **15**(4), p.3218.

Enrico Balugani, Rava, A. and Marazza, D. 2020. Variance based sensitivity analysis of the RUSLE model in the E.U. parameter space.

Estrada-Carmona, N., Harper, E.B., DeClerck, F. and Fremier, A.K. 2016. Quantifying model uncertainty to improve watershed-level ecosystem service quantification: a global sensitivity analysis of the RUSLE. *International Journal of Biodiversity Science, Ecosystems Services & Management*. **13**(1), pp.40–50.

Ferro, V. and Porto, P. 2000a. Sediment Delivery Distributed (SEDD) Mode. *Journal of Hydrologic Engineering*. **5**(4).

Ferro, V. and Porto, P. 2000b. Sediment Delivery Distributed (SEDD) Model. *Journal of Hydrologic Engineering*. **5**(4), pp.411–422.

Fontes De Maria, L. and Phillips, W. 2019. An economic analysis of flooding in the Caribbean: The case of Jamaica and Trinidad and Tobago. *Handle.net*. [Online]. [Accessed 15 August 2024]. Available from: https://hdl.handle.net/11362/44877.

Food and Agriculture Organisation 2007. FAO Map Catalog. *data.apps.fao.org*. [Online]. Available from: https://data.apps.fao.org/map/catalog/srv/eng/catalog.search#/metadata/446ed430-8383-11db-b9b2-000d939bc5d8.

GDAL Development Team. 2024. GDAL - Geospatial Data Abstraction Library. Open Source Geospatial Foundation. http://www.gdal.org

Gelagay, H.S. 2016. RUSLE and SDR Model Based Sediment Yield Assessment in a GIS and Remote Sensing Environment; A Case Study of Koga Watershed, Upper Blue Nile Basin, Ethiopia. *Journal of Waste Water Treatment & Analysis*. **7**(2).

Getu, L.A., Nagy, A. and Addis, H.K. 2022. Soil loss estimation and severity mapping using the RUSLE model and GIS in Megech watershed, Ethiopia. *Environmental Challenges*. **8**, p.100560.

Ghosal, K. and Das Bhattacharya, S. 2020. A Review of RUSLE Model. *Journal of the Indian Society of Remote Sensing*. **48**(4), pp.689–707.

Gianinetto, M., Aiello, M., Polinelli, F., Frassy, F., Rulli, M.C., Ravazzani, G., Bocchiola, D., Chiarelli, D.D., Soncini, A. and Vezzoli, R. 2019. D-RUSLE: a dynamic model to estimate potential soil erosion with satellite time series in the Italian Alps. *European Journal of Remote Sensing*. **52**(sup4), pp.34–53.

Gorelick, N., Hancher, M., Dixon, M., Ilyushchenko, S., Thau, D. and Moore, R. 2017. Google Earth Engine: Planetary-scale geospatial analysis for everyone. *Remote Sensing of Environment*. **202**, pp.18–27.

Harliando, D.P., Saputri, H.I., Setyawan, C., Khidzir, A., Susanto, S. and Zaki, M.K. 2022. RUSLE CP Factor Optimization for Soil Erosion Modeling in Tropical Watershed of Indonesia. *Advances in biological sciences research/Advances in Biological Sciences Research*.

Harris, C.R., Millman, K.J., van der Walt, S.J., Gommers, R., Virtanen, P., Cournapeau, D., Wieser, E., Taylor, J., Berg, S., Smith, N.J., Kern, R., Picus, M., Hoyer, S., van Kerkwijk, M.H., Brett, M., Haldane, A., del Río, J.F., Wiebe, M., Peterson, P. and Gérard-Marchant, P. 2020. Array Programming with NumPy. *Nature*. **585**(7825), pp.357–362.

Hurni, H. 1985. Erosion Productivity Conservation Systems in Ethiopia. Proceedings of 4th International Conference on Soil Conservation, Maracay, Venezuela, 3-9 November 1985, 654-674. - References - Scientific Research Publishing. *www.scirp.org*. [Online]. [Accessed 19 July 2024]. Available from: https://www.scirp.org/reference/referencespapers?referenceid=1813906.

Jaramillo, F., Cooper , V.A. and Gaskin, S.J. 2007. Estimating and modeling soil loss and sediment yield in the Maracas-St. Joseph River catchment with empirical models (RUSLE and MUSLE) and a physically based model (EROSION 3D). *escholarship.mcgill.ca*. [Online]. Available from: https://escholarship.mcgill.ca/concern/theses/st74ct43c.

Kavian, A., Hoseinpoor Sabet, S., Solaimani, K. and Jafari, B. 2016. Simulating the effects of land use changes on soil erosion using RUSLE model. *Geocarto International*. **32**(1), pp.97–111.

Kebede, Y.S., Endalamaw, N.T., Sinshaw, B.G. and Atinkut, H.B. 2021. Modeling soil erosion using RUSLE and GIS at watershed level in the upper beles, Ethiopia. *Environmental Challenges*. **2**, p.100009.

Kidane, M., Bezie, A., Kesete, N. and Tolessa, T. 2019. The impact of land use and land cover (LULC) dynamics on soil erosion and sediment yield in Ethiopia. *Heliyon*. **5**(12), p.e02981.

Kleinman, P. 1995. The ecological sustainability of slash-and-burn agriculture. *Agriculture, Ecosystems & Environment*. **52**(2-3), pp.235–249.

Kogo, B.K., Kumar, L. and Koech, R. 2020. Impact of Land Use/Cover Changes on Soil Erosion in Western Kenya. *Sustainability*. **12**(22), p.9740.

Laflen, J.M., Lane, L.J. and Foster, G.R. 1991. WEPP: A new generation of erosion prediction technology. *Journal of Soil and Water Conservation*. **46**(1), pp.34–38.

Loch, R. and Rosewell, C. 1992. Laboratory methods for measurement of soil erodibilities (K-factors) for the universal soil loss equation. *Soil Research*. **30**(2), p.233.

Lu, D., Li, G., Valladares, G.S. and Batistella, M. 2004. Mapping soil erosion risk in Rondônia, Brazilian Amazonia: using RUSLE, remote sensing and GIS. *Land Degradation & Development*. **15**(5), pp.499–512.

Lujan, D.L. and Gabriels, D. 2005. Assessing the Rain Erosivity and Rain Distribution in Different Agro-Climatological Zones in Venezuela. *Sociedade & Natureza*. **1**(1), pp.16–29.

Luvai, A., Obiero, J. and Omuto, C. 2022. Soil Loss Assessment Using the Revised Universal Soil Loss Equation (RUSLE) Model F. Lisetskii, ed. *Applied and Environmental Soil Science*. **2022**, pp.1–14.

Mallick, J., Alashker, Y., Mohammad, S.A.-D., Ahmed, M. and Hasan, M.A. 2014. Risk assessment of soil erosion in semi-arid mountainous watershed in Saudi Arabia by RUSLE model coupled with remote sensing and GIS. *Geocarto International*. **29**(8), pp.915–940.

Maracas Valley Action Committee 2010. *Issues Of Sustainable Development In Maracas Valley Trinidad & Tobago*. United Nations Development Programme .

Martínez-Murillo, J.F., Remond, R. and Ruiz-Sinoga, J.D. 2020. Validation of RUSLE K factor using aggregate stability in contrasted mediterranean eco-geomorphological landscapes (southern Spain). *Environmental Research*. **183**, p.109160.

McCool, D.K. 1987. Revised Slope Steepness Factor for the Universal Soil Loss Equation. *The American Society of Agricultural and Biological Engineers*.

Moisa, M.B., Negash, D.A., Merga, B.B. and Gemeda, D.O. 2021. Impact of land-use and land-cover change on soil erosion using the RUSLE model and the geographic information system: a case of Temeji watershed, Western Ethiopia. *Journal of Water and Climate Change*.

Moore, I.D. and Burch, G.J. 1986. Modelling Erosion and Deposition: Topographic Effects. *Transactions of the ASAE*. **29**(6), pp.1624–1630.

Morawitz, D.F., Blewett, T.M., Cohen, A. and Alberti, M. 2006. Using NDVI to Assess Vegetative Land Cover Change in Central Puget Sound. *Environmental Monitoring and Assessment*. **114**(1-3), pp.85–106.

Morgan, R.P.C., Quinton, J.N., Smith, R.E., Govers, G., Poesen, J.W.A., Auerswald, K., Chisci, G., Torri, D. and Styczen, M.E. 1998. The European Soil Erosion Model (EUROSEM): a dynamic approach for predicting sediment transport from fields and small catchments. *Earth Surface Processes and Landforms*. **23**(6), pp.527–544.

Mustefa, M., Fufa, F. and Takala, W. 2019. GIS estimation of annual average soil loss rate from Hangar River watershed using RUSLE. *Journal of Water and Climate Change*. **11**(2), pp.529–539.

NASA, METI, AIST, Japan Spacesystems and U.S./Japan ASTER Science Team 2019. ASTER Global Digital Elevation Model V003 [Data set]. Available from: https://doi.org/10.5067/ASTER/ASTGTM.003.

Nearing, M.A., Yin, S., Borrelli, P. and Polyakov, V.O. 2017. Rainfall erosivity: An historical review. *CATENA*. **157**, pp.357–362.

Negese, A., Fekadu, E. and Getnet, H. 2021. Potential Soil Loss Estimation and Erosion-Prone Area Prioritization Using RUSLE, GIS, and Remote Sensing in Chereti Watershed, Northeastern Ethiopia. *Air, Soil and Water Research*. **14**, 117862212098581.

Nel, W., Anderson, R.L., Sumner, P.D., Boojhawon, R., Rughooputh, S. and Dunputh, B. 2013. Temporal sensitivity analysis of erosivity estimations in a high rainfall tropical island environment. *Geografiska annaler. Series A, Physical geography/Geografiska annaler. Series A. Physical geography*. **95**(4), pp.337–343.

Nigel, R. and Rughooputh, S. 2010. Mapping of monthly soil erosion risk of mainland Mauritius and its aggregation with delineated basins. *Geomorphology*. **114**(3), pp.101–114.

Obiahu, O.H. and Elias, E. 2020. Effect of land use land cover changes on the rate of soil erosion in the Upper Eyiohia river catchment of Afikpo North Area, Nigeria. *Environmental Challenges*. **1**, p.100002.

Ouyang, W., Hao, F., Skidmore, A.K. and Toxopeus, A.G. 2010. Soil erosion and sediment yield and their relationships with vegetation cover in upper stream of the Yellow River. *Science of The Total Environment*. **409**(2), pp.396–403.

Panagos, P., Ballabio, C., Borrelli, P., Meusburger, K., Klik, A., Rousseva, S., Tadić, M.P., Michaelides, S., Hrabalíková, M., Olsen, P., Aalto, J., Lakatos, M., Rymszewicz, A., Dumitrescu, A., Beguería, S. and Alewell, C. 2015. Rainfall erosivity in Europe. *Science of The Total Environment*. **511**, pp.801–814.

Peters, E.J. 2015. The 2009/2010 Caribbean drought: a case study. *Disasters*. **39**(4), pp.738–761.

Qiao, X., Li, Z., Lin, J., Wang, H., Zheng, S. and Yang, S. 2023. Assessing current and future soil erosion under changing land use based on InVEST and FLUS models in the Yihe River Basin, North China. *International Soil and Water Conservation Research*.

Ragoobir, S. 2018. Planning For Climate Variability And Change Vulnerability Of The North Coast Of Trinidad Against Natural And Man-Made Threats [Online]. [Accessed 15 August 2024]. Available from: https://cwwa.net/wp/wp-content/uploads/2019/08/Vulnerability-of-the-North-Coast-of-Trinidad-Against-Natural-and-the-Man-Made-Threats-S.-Ragoobir.pdf.

Renard, K.G. 1997. Predicting Soil Erosion by Water A Guide to Conservation Planning with the Revised Universal Soil Loss Equation (RUSLE). Washington DC United States

Government Printing. - References - Scientific Research Publishing. *www.scirp.org*. [Online]. Available from: https://www.scirp.org/reference/referencespapers?referenceid=2770691.

Ricci, G.F., Jeong, J., De Girolamo, A.M. and Gentile, F. 2020. Effectiveness and feasibility of different management practices to reduce soil erosion in an agricultural watershed. *Land Use Policy*. **90**, p.104306.

Rodrigues, E., Vitor Matheus Bacani and Elói Panachuki 2017. Modeling soil erosion using RUSLE and GIS in a watershed occupied by rural settlement in the Brazilian Cerrado. *Natural Hazards*. **85**(2), pp.851–868.

Saggau, P., Kuhwald, M. and Duttmann, R. 2023. Effects of contour farming and tillage practices on soil erosion processes in a hummocky watershed. A model-based case study highlighting the role of tramline tracks. *CATENA*. **228**, p.107126.

Sahoo, P.K., Dall'Agnol, R., Salomão, G.N., da Silva Ferreira Junior, J., da Silva, M.S., Martins, G.C., e Souza Filho, P.W.M., Powell, M.A., Maurity, C.W., Angelica, R.S., da Costa, M.F. and Siqueira, J.O. 2019. Source and background threshold values of potentially toxic elements in soils by multivariate statistics and GIS-based mapping: a high density sampling survey in the Parauapebas basin, Brazilian Amazon. *Environmental Geochemistry and Health*. **42**(1), pp.255–282.

Seitz, S., Goebes, P., Puerta, V.L., Pereira, E.I.P., Wittwer, R., Six, J., van der Heijden, M.G.A. and Scholten, T. 2018. Conservation tillage and organic farming reduce soil erosion. *Agronomy for Sustainable Development*. **39**(1).

Sharma, A., Tiwari, K.N. and Bhadoria, P.B.S. 2010. Effect of land use land cover change on soil erosion potential in an agricultural watershed. *Environmental Monitoring and Assessment*. **173**(1-4), pp.789–801.

Sidi Almouctar, M.A., Wu, Y., Zhao, F. and Dossou, J.F. 2021. Soil Erosion Assessment Using the RUSLE Model and Geospatial Techniques (Remote Sensing and GIS) in South-Central Niger (Maradi Region). *Water*. **13**(24), p.3511.

Singh, B. 1997. Climate-related global changes in the southern Caribbean: Trinidad and Tobago. *Global and Planetary Change*. **15**(3-4), pp.93–111.

Sourn, T., Pok, S., Chou, P., Nut, N., Theng, D. and Prasad, P.V.V. 2022. Assessment of Land Use and Land Cover Changes on Soil Erosion Using Remote Sensing, GIS and RUSLE Model: A Case Study of Battambang Province, Cambodia. *Sustainability*. **14**(7), p.4066.

Stanchi, S., Freppaz, M., Ceaglio, E., Maggioni, M., Meusburger, K., Alewell, C. and Zanini, E. 2014. Soil erosion in an avalanche release site (Valle d'Aosta: Italy): towards a winter factor for RUSLE in the Alps. *Natural Hazards and Earth System Sciences*. **14**(7), pp.1761–1771.

Strohbach, M.W., Döring, A.O., Möck, M., Sedrez, M., Mumm, O., Schneider, A.-K., Weber, S. and Schröder, B. 2019. The 'Hidden Urbanization': Trends of Impervious Surface in Low-Density Housing Developments and Resulting Impacts on the Water Balance. *Frontiers in Environmental Science*. **7**.

Thapa, P. 2020. Spatial estimation of soil erosion using RUSLE modeling: a case study of Dolakha district, Nepal. *Environmental Systems Research*. **9**(1).

Trinidad and Tobago Meteorological Service 2024. Climate. *www.metoffice.gov.tt*. [Online]. Available from: https://www.metoffice.gov.tt/Climate.

Tsihrintzis, V.A., Hamid, R. and Fuentes, H.R. 1996. Use of Geographic Information Systems (GIS) in water resources: A review. *Water Resources Management*. **10**(4), pp.251–277.

Usman, M., Liedl, R., Shahid, M.A. and Abbas, A. 2015. Land use/land cover classification and its change detection using multi-temporal MODIS NDVI data. *Journal of Geographical Sciences*. **25**(12), pp.1479–1506.

Valor, E. 1996. Mapping land surface emissivity from NDVI: Application to European, African, and South American areas. *Remote Sensing of Environment*. **57**(3), pp.167–184.

Veldkamp, E., Schmidt, M., Powers, J.S. and Corre, M.D. 2020. Deforestation and reforestation impacts on soils in the tropics. *Nature Reviews Earth & Environment*. **1**(1), pp.1–16.

Williams, J.R. and Sharpley, A.N. 1990. EPIC-erosion/productivity impact calculator: 1. Model documentation. *Technical Bulletin - United States Department of Agriculture*.

Yu, B. and Rosewell, C. 1996. Rainfall erosivity estimation using daily rainfall amounts for South Australia. *Soil Research*. **34**(5), p.721.

Zhang, H., Yao, Z., Yang, Q., Li, S., Baartman, J.E.M., Gai, L., Yao, M., Yang, X., Ritsema, C.J. and Geissen, V. 2017. An integrated algorithm to evaluate flow direction and flow accumulation in flat regions of hydrologically corrected DEMs. *CATENA*. **151**, pp.174–181.

Zhou, P., Luukkanen, O., Tokola, T. and Nieminen, J. 2008. Effect of vegetation cover on soil erosion in a mountainous watershed. *CATENA*. **75**(3), pp.319–325.

Zingg, W. 1940. Degree and length of land slope as it affects soil loss in runoff. *Agricultural Engineering*. **21**, pp.59–64.

Appendix

Link to OneDrive:

GEOG5160